Surface Energy Balance on the Arctic Tundra: Measurements and Models

A. H. LYNCH,* F. S. CHAPIN III,+ L. D. HINZMAN,# W. WU,* E. LILLY,#
G. VOURLITIS,@ AND E. KIM&

* *Cooperative Institute for Research in the Environmental Sciences, University of Colorado, Boulder, Colorado*
+ *Institute of Arctic Biology, University of Alaska, Fairbanks, Alaska*
# *Water and Environmental Research Center, University of Alaska, Fairbanks, Alaska*
@ *Global Change Research Group, San Diego State University, San Diego, California*
& *Department of Electrical Engineering, University of Michigan, Ann Arbor, Michigan*

(Manuscript received 20 July 1998, in final form 13 October 1998)

ABSTRACT

The progress made in the Land–Atmosphere–Ice Interactions Flux Study over the past 4 yr to fully characterize the biophysical fluxes in the snow-free tundra ecosystem and their relationship to climate and climate change is described. This paper is the result of a synthesis effort to bring together the measurements of surface fluxes at various sites on the North Slope of Alaska in the snow-free period of 1995 with the results of modeling efforts for this region. It is found that methodological and site dissimilarities contribute to measurement differences at least as much as instrument and sampling error, even for closely collocated and similarly vegetated sites. The regional climate model employed in this study generally simulates fluxes that are within the range of measured fluxes, but tends to overestimate both net radiation and latent heat fluxes. The regional model also captures site to site variations quite well, which appear to be more sensitive to mesoscale meteorological conditions than on specifics of site characteristics. The active layer model employed in this study performs well in estimating ground heat flux but rather more poorly in simulating turbulent fluxes. The global climate model is unable to capture the broad-scale response of the land surface sensible heat flux and net radiation, although it performs rather better in the simulation of latent and ground heat fluxes. Finally, the intended purposes and applications of both data and model simulations have a strong impact on their applicability to other studies.

1. Introduction and historical perspective

Although the surface energy balance is of fundamental importance to meteorological, hydrological, geomorphological, and ecological processes, the controls over the surface energy balance and its relationship to climate have not been well characterized for arctic and alpine tundra ecosystems. Greater attention has been paid to tropical environments (e.g., Henderson-Sellers and Gornitz 1984; Nobre et al. 1991) and boreal forest, particularly the relationship between the northern treeline and climate (Bonan et al. 1995; Lafleur et al. 1992; Foley et al. 1994). The northern treeline represents an abrupt change in surface characteristics and microclimate, from the high leaf area index, tall, deeply rooting boreal forest to the low leaf area index, shallow rooting and short stature of tundra grasses and shrubs. However, the location of the boreal forest–tundra transition zone is not the only factor to consider when examining the influence of the tundra ecosystem upon climate—representation of key features of this ecosystem, including vegetation characteristics, permafrost, and surface standing water, is necessary for the relationship between tundra and climate to be adequately treated in predictions of climate (Wilson et al. 1987). This relationship is a problem not of the influence of vegetation on climate, but of the dynamic interplay between climate, vegetation, and soils (Hare and Ritchie 1972; Pielke and Vidale 1995).

Arctic ecosystems (tundra and boreal forest) have received considerable attention in the global budgets of carbon dioxide and methane, since arctic soils and peatlands have large stores of carbon (Post et al. 1982) and are important sources and sinks of these gases. The biogeochemical processes that control the carbon budget are sensitive to local changes in soil moisture and temperature (Oechel et al. 1993; Whalen and Reeburgh 1990). Therefore, any changes in surface energy exchange that alter these soil parameters could have profound effects on trace-gas feedbacks to climate. Vegetation redistribution, and especially movement of the treeline, in response to changes will also have a dramatic impact upon these processes (Smith and Shugart 1993). Long-term observations in interior Alaska show that the patchy and discontinuous permafrost is presently thaw-

Corresponding author address: Dr. Amanda H. Lynch, CIRES, Campus Box 216, University of Colorado, Boulder, CO 80309.
E-mail: manda@cires.colorado.edu

ing (Osterkamp 1994), which represents a positive feedback for atmospheric carbon dioxide increase. However, these responses are climatically important only at long temporal scales (Graetz 1991). Biophysical land–atmosphere coupling via albedo, interactions between vegetation and snow, and modulation of the sensible and latent heat fluxes, have important climatic implications on seasonal to decadal timescales (Otterman et al. 1984; Harvey 1988b; Thomas and Rowntree 1992; Bonan et al. 1992). In concert with boreal forest, the effects of tundra extend to the subarctic, and over longer timescales, even to the Tropics (Bonan et al. 1992, 1995; Alley 1995).

While the role of the boreal forest in the climate system has been relatively well characterized in both empirical and modeling studies (Goulden et al. 1997; Baldocchi et al. 1997), studies of the surface energy balance of the arctic tundra, especially permafrost-dominated tundra in Alaska, have been limited until the National Science Foundation Arctic System Science Program, Land–Atmospheric–Ice Interactions (LAII) Flux Study (LAII Science Steering Committee 1997). The first thorough energy balance measurements for tundra were made around the time of the International Geophysical Year in Alaska (Mather and Thornthwaite 1956, 1958). More intensive observations followed in Alaska (Wendler 1967; Weller and Benson 1971; Weller and Holmgren 1974) and the Canadian Arctic (Vowinckel 1966; Ahrnsbrak 1968) and particularly radiation measurements in the Russian Arctic [see Ohmura (1982a) for extensive references]. More recently, partitioning of turbulent energy fluxes had been measured in several sites, especially in the Canadian Arctic, with a view to characterizing the differences between boreal forest and tundra (Lafleur and Rouse 1995). By the time of the LAII Flux Study, the radiative energy exchange on Alaskan coastal tundra was relatively well understood with the exception of cloud–radiation interactions, but no single project had been continued long enough to be climatologically reliable, or had considered variations among tundra types. This paper presents the progress made in the LAII Flux Study over the past 4 yr to fully characterize the biophysical fluxes in the snow-free tundra ecosystem and their relationship to climate. Section 2 presents a review of the high-latitude summertime energy balance over tundra, and section 3 discusses different types of modeling approaches. Section 4 presents a synthesis of the results of measurements and modeling performed as part of the LAII Flux Study for the growing season of 1995, and section 5 summarizes the advances made in understanding by this work.

2. Recent measurement of the surface energy balance over tundra

Prior to the LAII Flux Study, most recent measurements of the surface energy balance were made in the Canadian Arctic. Much of the effort was aimed at understanding the position of the northern treeline, rather than an examination in detail of the tundra ecosystem. Ohmura (1982b) is one exception to this, having measured the seasonal characteristics of the surface energy balance over tundra alone during the snow-covered, melt and post-melt periods at Axel Heiberg Island, Northwest Territories, Canada. Results from these measurements, performed in 1969 and 1970, were compared with historical databases compiled for Barrow (and shown in Table 2) and with the surface energy balance over the Arctic Ocean and glaciers. Compared with these surfaces, the tundra is warmer, with a larger diurnal temperature range, less cloud cover, and lower wind speeds.

Measurements in the Hudson Bay region from several growing seasons (Rouse et al. 1992) showed that evaporative flux tended to be large during dry conditions, with a more rapid downward thaw than during moist conditions. In contrast, Riseborough and Burn (1988) reported that, in subarctic moss-forest in the Yukon, the moisture in the organic layer is decoupled from the mineral soil beneath, so that evaporation declines through the summer. This reduces thermal conductivity of the organic layer so that the mineral soils remain cold. In the tundra measurements, the underlying peat remained moist even though the water table was well beneath the surface. The Hudson Bay results also contrast with measurements of alpine tundra in the Rocky Mountains, Canada, where summertime Bowen ratios were consistently greater than unity for dry days and very close to unity for moist days (Bowers and Bailey 1989) as in other alpine tundra measurements (Isard and Belding 1989; Shaeffer and Reiter 1987). These results suggest that arctic tundra might have higher evaporative fluxes than boreal or alpine sites.

In work comparing the behavior of contiguous wetland tundra and forest, Lafleur and Rouse (1995) found in measurements from 286 summer days over 5 yr in the Hudson Bay region that average Bowen ratios were 0.45 for tundra, and 0.66 for forest, and that Bowen ratios were consistently higher for forest, due to both larger sensible heat fluxes and lower latent heat fluxes. They used the contrast between cool moist marine winds and warm dry continental winds as an analog for changing climate, since they had documented that energy partitioning is strongly influenced by wind direction (Lafleur and Rouse 1988). They found that the surface energy balance over tundra was more sensitive to changing wind conditions than the forested site. However such an analogy is limited since it ignores long-term changes in the land surface–vegetation system. An alternative analog is used in Rouse et al. (1992), who suggest that selecting the behavior of hot dry growing seasons from a multiyear dataset can represent a more likely regime in the future. The difficulty of this approach is that it is not clear that summers in the future will be drier in this region.

There is considerable variation even among different

tundra types. Rott and Obleitner (1992) performed energy balance measurements over dry tundra in west Greenland for 4 weeks of the growing season of 1988. The energy balance in this region was strongly influenced by air temperature, which was defined by topographic effects and by the proximity of the ice cap with its katabatic flow. They found good agreement between the turbulent fluxes derived from the Bowen ratio method and by the aerodynamic method. In this case the Bowen ratio was generally greater than unity and often reached as high as 3. The exceptions to this were periods immediately following a precipitation event, when wet soils increased the latent heat fluxes. Transpiration from vegetation added little to the transport of humidity from the soil to the air, since the vegetation was sparse and largely dormant. The drying of the top soil layer restricted evaporation and preserved water in the soil. Thus, this tundra behaved more like alpine tundra than the wetland tundra of Hudson Bay and Barrow.

Harazono et al. (1996) found that energy partitioning at their coastal site near Prudhoe Bay, Alaska, was strongly controlled by cold and warm air advection as observed near the Hudson Bay coast (Lafleur and Rouse 1995). Onshore winds advected cold and humid air masses from the Arctic Ocean resulting in low air temperature, a large temperature gradient between the land surface and the air, and therefore a high sensible heat flux and low evaporative flux. Conversely, when offshore winds advected warm and dry continental air to the site, the temperature gradient between the land surface and air was small, resulting in low sensible heat flux, but only slightly higher evaporative flux than during onshore wind conditions. The difference in energy partitioning was primarily due to larger heat gain of the open water ponds during the offshore conditions and to a minor increase in ground heat flux. Yoshimoto et al. (1996) found a similar behavior in energy partitioning at Barrow, Alaska, during their 1993 field season. When the tundra surface was dry, the relative fraction of net radiation dissipated to sensible heat increased with wind speed while the fraction dissipated to latent heat did not. Only after rain events with standing water did the fraction of net radiation dissipated to latent heat flux increase with wind speed. This finding is in agreement with Ohmura (1984), who noted that the relative importance of latent heat flux depends more on the frequency of the advection of the maritime air mass than on the soil water content.

3. Representation of the land surface in models

Some representation of the land surface and vegetation is required in any model of water and energy exchange, including hydrology models, energy balance models, and global and regional models used to simulate weather and climate. In many instances, climate models regard the land surface as relatively constant, and similarly in ecosystem and hydrologic models, the climate is considered an external parameter. In this section we will summarize the approaches taken in the various classes of models, and the progress toward integration.

The interplay between arctic hydrologic processes and surface–atmosphere fluxes of water and energy is a complex problem, but essential for a complete understanding of the regional surface energy balance. Models have been developed that treat certain components of the hydrologic system, such as conceptual watershed models (e.g., Bergstrom 1986), stochastic models (e.g., Shaw 1994), and physically based, spatially distributed models (e.g., Beven and Kirkby 1979; Zhang et al. 1999). The summertime tundra represents a unique problem, due to the presence of continuous permafrost, acting as an impermeable layer to subsurface flow, and to the freeze–thaw cycle of the active layer, which yields a constantly changing lower–boundary condition. Most current simulations of arctic hydrologic processes use lumped-parameter models, which simulate the total response of a particular water basin (Hinzman and Kane 1992).

Rouse et al. (1992) represented the surface energy balance of sedge wetland tundra in summer using a ''box'' model consisting of vegetation, soil, and the lower 2 m of the atmosphere. The bottom of the box interfaced with the water table. Using measurements of precipitation, net radiation, soil heat flux, the atmospheric profiles of temperature, water vapor pressure, and wind, the model predicted sensible and latent heat fluxes from the ground, evapotranspiration from the vegetation (using the Penman–Monteith model; Monteith 1965), and soil temperature and moisture. Even though this model is heavily data dependent, Rouse et al. (1992) were able to perform experiments to assess the impact of changed climatic forcing on the tundra ecosystem. They suggest that, because soil is completely saturated after the spring thaw, there is no memory of a previous season's dryness, and hence a warmer climate with a longer growing season, even if dryer, will produce infilling of sedges giving a larger leaf area index. Thus, this positive feedback tends to increase the significance of vegetation characteristics in a warmer climate.

Energy balance models (EBMs) were the earliest attempts to represent the climate of the globe. In their simplest form, EBMs are zero-dimensional balances between incoming solar and outgoing longwave radiation, and predict a global average temperature. However, recognition of the need to include the important energetic feedbacks led to more sophisticated treatments, some of which take into account latitudinal zones. For example, Harvey (1988a) developed an EBM with up to 2.5° latitude resolution, and explicit representations of sea ice, snow, clouds, and 10 vegetation categories. Harvey (1988b) concluded that the climate feedbacks associated with the masking of snow by vegetation, the hydrologic processes, and the location of the northern treeline were of much smaller importance than suggested by results

of other authors using more sophisticated models (Otterman et al. 1984; Wilson et al. 1987). The sensitivity of climate to these factors has since been demonstrated by experiments that include explicitly three-dimensional representations of land, oceans, sea ice, and atmosphere (e.g., Thomas and Rowntree 1992; Bonan et al. 1995). This illustrates the difficulties in using simple energy balance models to represent the sensitivity of the climate system.

Recently, increased emphasis has been placed on the proper biophysical parameterization of the mechanisms that regulate the fluxes of water vapor and energy over the land surface in global climate models. These parameterizations [e.g. Bonan 1996 (Land Surface Model, LSM); Dickinson et al. 1993 (Biosphere–Atmosphere Transfer Scheme, BATS); Sellers et al. 1986 (Simple Biosphere Model, SiB); Verseghy 1991; Verseghy et al., 1993 (Canadian Land Surface Scheme, CLASS)] represent the heterogeneous soil and vegetation-covered land surface in a range of detail and sophistication, but all employ some representation of vegetation characteristics and soil heat transfer and hydrology. Vegetation and the soils that support them are intimately intertwined and their relative impacts are not easily distinguished. Many formulations employ the analogy of a ''big leaf,'' which assumes that the vegetation within a grid cell is distributed uniformly so that all physical and biological processes need be modeled in one dimension (vertical) only. This ''big leaf'' does not correspond to any specific plant, but rather represents a composite of the vast array of plants making up a particular type of ecosystem (e.g., tundra, savanna, tropical rainforest). The processes generally represented include momentum transfer, evapotranspiration, radiant and turbulent energy exchange, and soil thermodynamic and hydrologic processes in the root zone and in some specified deeper soil layers or reservoir. In some cases, the physical models have been supplemented by assimilating directly measured or remotely sensed data (e.g., Smith et al. 1993). Such models have also been used in ''standalone'' mode, that is, forced by observed atmospheric conditions at a single point, rather than interacting spatially with a simulated atmosphere. Tilley and Lynch (1998) found that several commonly used models (BATS, LSM, and CLASS) varied widely in their simulations of soil temperature, soil moisture, and surface energy balance over tundra, even with identical forcing. Such differences highlight the importance of model formulation details such as parameter choice, number of soil layers, specification of soil textures, and description of vegetation characteristics.

Heterogeneity in meteorologically significant properties (e.g., heat capacity, wetness, albedo) results in variations in net radiation and partitioning of turbulent fluxes that cannot be ignored (Lafleur and Rouse 1995; Pielke et al. 1993). The nonlinear problem of representing the heterogeneity of the surface within a grid cell has been addressed in several ways, either as a linear combination of the surface energy and moisture balances of different types of composite ''big leaves'' within a grid cell (Avissar and Pielke 1989; Wetzel and Chang 1988), or as a linear combination of the fluxes from ''big leaves,'' which represent specific plant types (Bonan 1996). This latter approach is attractive in that measurements in the field can be linked more directly with model parameters. However, Pitman (1991) found that use of aggregate parameters to represent subgrid-scale heterogeneity did produce improved simulations, whereas incorporation of explicit representations of lakes or precipitation processes improved the level of realism but not necessarily the skill (i.e., congruence with observations) of the simulation. Pitman (1991) also points out that the surface responds in nonlinear ways to the addition of small amounts of forest to a tundra ecosystem, for example, especially with regard to the effects on momentum transfer and snowmelt.

Recently, some global climate studies have been extended to incorporate predictions of ecosystem distribution—essentially closing the feedback loop between climate and vegetation (Prentice et al 1992; Alcamo et al. 1994; Steffen et al. 1996). The simplest of these schemes is a life zone classification system (e.g., Holdridge 1964; Woodward 1987) in which climatic indices that incorporate such factors as total annual precipitation, mean annual temperature, and soil water deficit are used as proxies for ecosystem type. However, such schemes are based entirely on the current correlations of vegetation with climate, and hence, while they produce good agreement for present-day conditions (e.g., Emanuel et al. 1985), the results for future climate scenarios can provide only tentative guidance. For instance, Henderson-Sellers (1991) found that changed vegetation distributions due to a $2 \times CO_2$ scenario were smaller than those expected from clearing of land for agriculture and urbanization. In addition, such schemes are heavily dependent upon the accurate simulation of quantities such as precipitation, which is especially difficult in the high latitudes. The lack of agreement between GCM simulations and observed climate at high latitudes could be due to a combination of several factors. First, while GCM performance for the polar regions has improved dramatically in recent years (e.g., Bromwich et al. 1994; Maslanik et al. 1996), most discussions of likely climate changes are still based on the early-generation models that do not adequately treat high-latitude processes (Chen et al. 1995; Walsh and Crane 1992) or ecosystem dynamics. Second, the inability of GCMs to represent these processes may lead investigators to search for the wrong types of signals in observations, or existing datasets may not be adequate to show the types of changes predicted.

Studies of the effects of tundra on climate in general circulation models have been relatively sparse. Wilson et al. (1987) linked the anomalously high surface temperatures simulated in the National Center for Atmospheric Research (NCAR) Community Climate Model

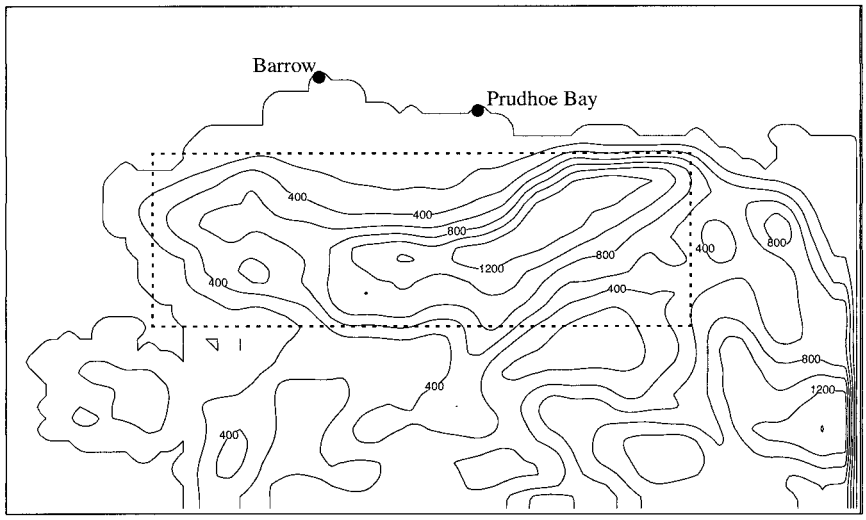

FIG. 1. North Slope of Alaska showing topography in m, covering the computational domain of the ARCSyM-3D model. The grid is 20-km resolution, and hence domain contains a total of 3375 grid boxes. Also shown (dotted box) is the CCM3 grid box used in this study.

(CCM) to shortcomings in the representation of the land surface. While little response to factors such as vegetation cover, root distribution, soil albedo, and active-layer depth was found, considerable sensitivity to the soil moisture was evident and highlighted the need to explicitly include permafrost to improve the simulation of soil hydrological processes. Bonan et al. (1995) employed another NCAR climate model, GENESIS, to examine the role of tundra and boreal forest in the climate system, and found that the most crucial factor was the location of the northern treeline, a relatively long timescale effect. In regional climate models, the influence of tundra has been examined only, to these authors' knowledge, in Lynch et al. (1998, 1999), in which it was found that vegetation-snow radiative feedbacks, soil thermal properties, and plant properties were crucial for a detailed simulation of spring and summer conditions in Alaska.

4. Results of measurements and modeling in the LAII flux study: 1995

This section presents the results of a synthesis effort to bring together the measurements of surface fluxes at various sites on the North Slope of Alaska in the snow-free period of 1995 with the results of modeling studies for this region. Section 4a describes the sites, measurement programs, and methods employed to derive surface fluxes as part of the LAII Flux Study, and section 4b describes the models used. Section 4c presents a comparison of measurement techniques for two sites characterized by different tundra vegetation, soils, and elevation. Section 4d discusses the site data in comparison with modeling and examines scaling issues associated with spatially explicit modeling results.

a. Measurement programs

Measurements were made by four groups at a site near Prudhoe Bay (70°16′47″N, 148°53′44″W, elevation 14 m) designated the Betty Pingo site. This site is located in a wetlands complex with little topographic relief with slopes of approximately 0.2%. The active layer is on average 40–50 cm in depth. Approximately 78% of the study area is characterized as a wetland (Rovansek et al. 1996). The dominant landforms in the wetland area are low-centered polygons, strangmoor ridges, and many small thaw ponds less than 1 m in depth. The remaining 22% of the study area is slightly higher (about 1 m) and is a drier, better-drained upland tundra dominated by high-centered polygons and ice wedges. The vegetation is dominated by sedges, mainly *Carex* and *Eriophorum* species with an average height of 10–15 cm. In the drier upland areas the sedges are intermixed with lichen, mosses, dwarf *Salix* and *Betula* species, and a variety of flowering herbaceous species (Walker et al. 1989; Rovansek et al. 1996). The soils are a complex of *Pergelic Cryosaprists*, *Pergelic Cryohemists*, and *Pergelic Cryaquepts* (Ping et al. 1994; Rovansek et al. 1996).

A second measurement site was established at Sagwon Bluffs (69°25′34″N, 148°41′24″W, elevation 300 m), approximately 100 km south of Betty Pingo. This site is located in a transitional zone between the coastal plain and the foothills. Measurements were collected near the top of the gently rolling hills on a 3% north-facing slope. The vegetation is characteristic of tussock tundra and the soils (*Pergelic Cryaquepts*) are loamy with a peaty surface layer and are poorly drained (Everett 1980). Figure 1 shows the topography of the North Slope of Alaska, and Fig. 2 shows the locations of these

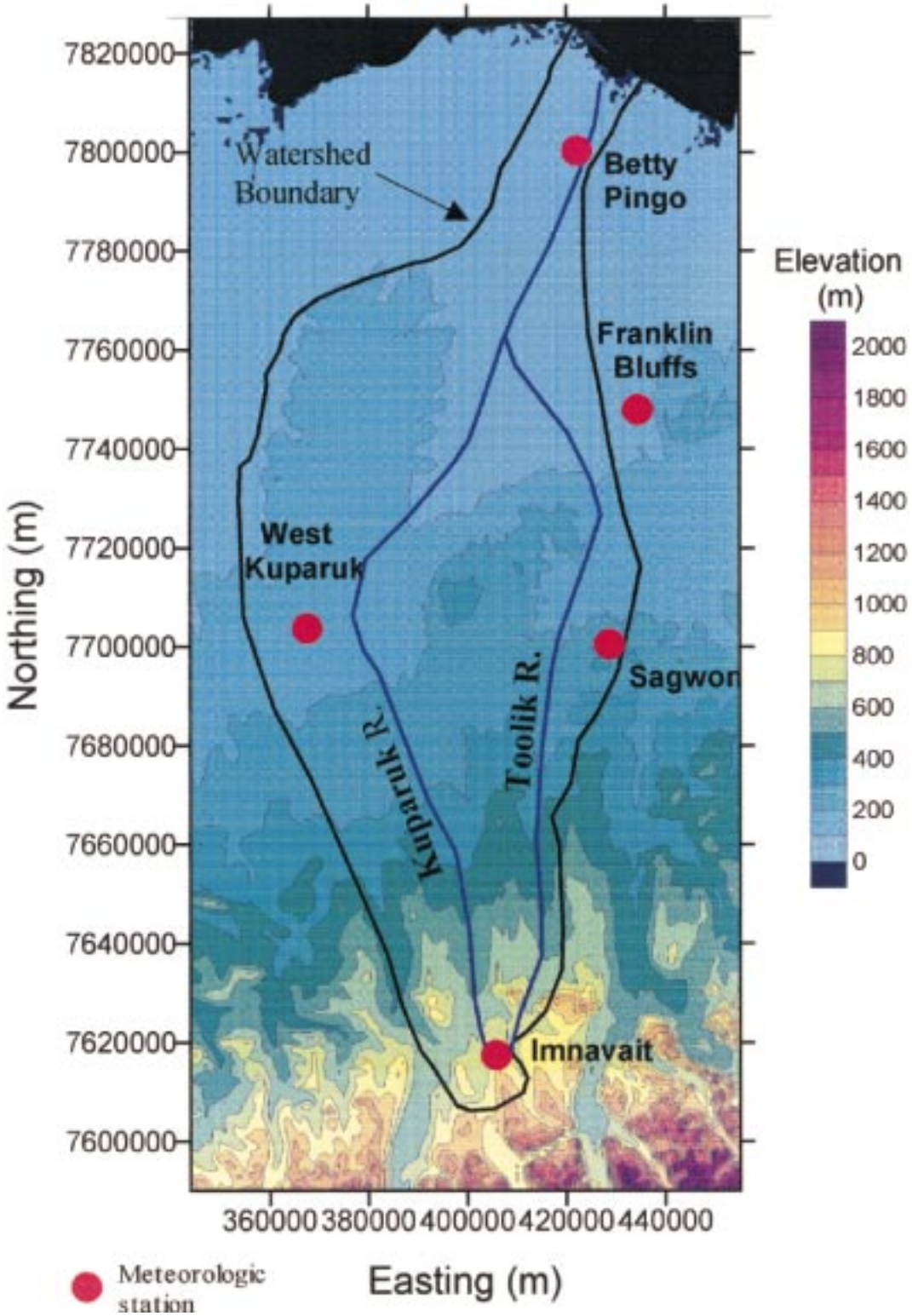

FIG. 2. Kuparuk River watershed showing topography in m and field site locations, covering the computational domain of the active-layer model.

TABLE 1. (a) Coastal sites (Betty Pingo, 70°18′N, 149°55′W). (b) Upland sites (Sagwon, 69°25′N, 148°45′W).

	Chapin and Eugster	England and Kim	Kane and Hinzman	Oechel and Vourlitis
a. Coastal sites				
Site information	Elevation: 12-m Vegetation: moist non-acidic grassy tundra	NA	Elevation: 30 m Vegetation: moist non-acidic grassy tundra	Elevation: 85 m Vegetation: moist non-acidic grassy tundra
Measurement period	1 July–8 July 30-min interval	NA	1 June–31 August 60-min interval	16 June–31 August 30-min interval
Quantities measured	Net radiation, albedo, air temperature, sensible and latent heat flux, ground heat flux, momentum flux, Bowen ratio, soil temperature, mean wind speed, roughness length, frictional velocity, humidity, air density, air pressure, carbon dioxide flux, and photosynthetic photon flux density.	NA	Air temperature, relative humidity, wind speed, wind direction, precipitation, soil temperatures, atmospheric longwave, terrestrial longwave, incident shortwave, reflected shortwave, and net radiation.	Net radiation, air temperature, sensible and latent heat flux, ground heat flux, wind direction, mean wind speed, frictional velocity, carbon dioxide flux, and photosynthetic photon flux density.
b. Upland sites*				
Site information	Elevation: 360 m Vegetation: mesic acidic tussock tundra	Elevation: 500 m Vegetation: mesic acidic tussock tundra	Elevation: 224 m Vegetation: mesic acidic tussock tundra	Elevation: 224 m Vegetation: mesic acidic tussock tundra
Measurement period	21 June–30 June 30-min interval	1 January–10 August 20–30-min interval	1 June–31 August 60-min interval	16 June–31 August 30-min interval
Quantities measured	Net radiation, albedo, air temperature, sensible and latent heat flux, ground heat flux, momentum flux, Bowen ratio, soil temperature, mean wind speed, roughness length, frictional velocity, humidity, air density, air pressure, carbon dioxide flux, and photosynthetic photon flux density.	Net radiation, air temperature, ground heat flux, soil temperature, precipitation, wind direction, mean wind speed, humidity.	Air temperature, relative humidity, wind speed, wind direction, precipitation, soil temperatures, atmospheric longwave, terrestrial longwave, incident shortwave, reflected shortwave, and net radiation.	Net radiation, air temperature, sensible and latent heat flux, ground heat flux, wind direction, mean wind speed, frictional velocity, evapotranspiration, carbon dioxide flux, and photosynthetic photon flux density.

* Note that England and Kim collected their data at Sagavanirktok River, 100 km south of Sagwon.

two sites, as well as several other measurement sites used for comparison with model simulations in section 4d. The details of the measurement programs at the two sites, Betty Pingo and Sagwon, including periods and quantities measured by each group, are given in Table 1. In addition, the climatological surface energy balance from Barrow (see Fig. 1) compiled by Ohmura (1982b) is included for comparison with the Betty Pingo site. This climatology was based on the data of Mather and Thornthwaite (1958), Maykut and Church (1973), and Weller and Holmgren (1974) and covers the years from 1957 to 1971. The Barrow site is a wet meadow tundra site with an elevation of 10 m, and is located about 350 km northwest of Betty Pingo.

The Chapin and Eugster group (Eugster et al. 1997) employed mobile eddy correlation towers to provide a basis for regional extrapolation of surface fluxes, which are sensitive to microscale variations in topography, vegetation and soils, and to measurement technique. This technique was applied to 25 sites on the North Slope of Alaska, including lowland and upland tundra in the coastal plain and foothills for the growing seasons of 1994–96 (19 June–14 August). Measurements at each site were generally carried out over a period of 7–10 days (see Table 1). Net radiation was measured with a net radiometer with an instrument accuracy of 5%. Both sensible and latent heat fluxes were measured by eddy covariance, using a 3-axis ultrasonic anemometer (10-Hz sampling frequency). Latent heat fluxes include both turbulent flux and a mesoscale flux component due to a mean vertical movement of air from coast to mountains during the summer period. Ground heat flux was measured with four heat-flux plates and were corrected for heat storage in the soil above the plates. Measurement error of the biophysical fluxes using this method was in the range 6%–9% for sensible, evaporative, and

ground heat fluxes. Differences in weather conditions or phenology between measurements made at different times or places, and different lengths of data record, contribute additional error. Consequently, we assume that only those fluxes that differ by more than 20% are truly different (Eugster et al. 1997).

Permanent towers were used by the Oechel and Vourlitis group to measure fluxes, water, and energy during June–August 1995 at the two sites for almost the entire measurement period (Vourlitis and Oechel 1997; Vourlitis 1997; Harazono et al. 1996). Measurements of sensible heat, latent heat, and carbon dioxide flux were by eddy covariance and ground heat flux by heat flux plates, using similar equipment to the Chapin and Eugster study. Net radiation was measured using a net radiometer, and basic meteorological measurements were also performed at the towers. Vourlitis and Oechel (1997) show an accuracy of within 3%–13% using the energy balance closure assessment.

The Kane and Hinzman group employed 10-m meteorological towers at the two sites (as well as five other sites to be discussed in section 4d; Hinzman et al. 1998; Mendez et al. 1998). Air temperature (typical accuracy 0.2°C), relative humidity (5%, with a self-aspirating radiation shield), wind speed (0.1 m s^{-1}), and direction (5°) were measured at each tower. These were the most reliable meteorological measurements available in this study. Fluxes were calculated from these measurements using an aerodynamic method. Soil temperatures were also measured, using thermistors, and surface temperatures were calculated using emitted longwave radiation measurements. Radiation instruments (net radiometers, pyranometers, and pyrgeometers) were installed in the spring and were usually taken down in the fall. Since these are remote, unmanned sites, rime ice, snowfall, and freezing precipitation can obscure the sensors in these instruments. Hence, values reported during periods of below freezing air temperature are questionable, and measured radiation values during winter, early spring, and fall should be considered qualitative and not quantitative.

The England and Kim group participated in the measurement of net radiation and ground heat flux, but not turbulent fluxes, from a single site adjacent to the Sagavanirktok River in the foothills of the Brooks Range (Kim and England 1995; see Table 1). This site was closer to the Dalton Highway (the main artery running from Fairbanks to Prudhoe Bay) than the Sagwon site described above. Local snowmelt progresses outward from the road, so an earlier melt and warming were experienced at this site, of approximately 1 week. However, snowmelt occurred in the first week of May, and hence its impact upon this comparison is probably small. The instruments were deployed on a flat moist acidic tussock tundra area adjacent to an abandoned gravel pad. All of the data was collected using a tower mounted aspirated net radiometer system, developed at the University of Michigan. The subsurface heat flux was measured using three heat flux plates. While the measurement program continued until 15 September, instrument failure meant that net radiation data was not available after 10 August.

b. Modeling programs

The results from two LAII modeling efforts (Hinzman et al. 1998; Lynch et al. 1995) were used in this synthesis—the active-layer thermal model and the Arctic Region Climate System Model (ARCSyM). Although the models differ markedly in purpose and structure, the overlap in the spatial and temporal domains of the simulations enable a useful comparison to each other and to field measurements collected during the campaign.

1) ACTIVE-LAYER MODEL

In support of hydrologic modeling efforts of the LAII Flux program, it was necessary to develop a spatially distributed model of active-layer processes. Correct simulation of hydrologic processes such as surface and subsurface runoff, evapotranspiration, and soil moisture dynamics are critically dependent upon correctly simulating the thickness of the active layer. This model is based upon solution of equations of the surface energy balance to obtain the surface temperature. This temperature is then used to drive a subsurface heat conduction and phase change model in determination of the subsurface temperature profile and depth of thaw (Hinzman et al. 1998). The spatial resolution of the simulation was nominally 1 km and the domain is shown in Fig. 2.

The subsurface thermal dynamics may be simulated quite accurately if the surface temperature is provided and the soil thermal properties are known (Kane et al. 1991). The surface temperature is the most important variable in the solution of the surface energy balance equation as each of the interacting processes of the surface energy balance maintain a dynamic equilibrium with fluxes controlled by the magnitude of the surface temperature. The effective surface temperature was determined for each node by solving the surface energy transfer equations simultaneously. This value of effective surface temperature was then used to drive the subsurface thermal model to calculate the temperature profile and depth of thaw. The surface energy balance is calculated from the net radiation, sensible and latent heat fluxes, and subsurface heat conduction. Turbulent fluxes are calculated using a simple exchange coefficient technique with a Richardson number adjustment for atmospheric stability. The soil heat flux is calculated using the Fourier heat conduction equation. Each equation that describes a single component of the surface energy balance includes the surface temperature as a variable. All of these can be assembled into a single nonlinear equation for the surface temperature. At each time step this equation was generated using measured meteorological data and then solved for the surface temperature. The

TABLE 2. LAII Flux Study sites for model comparison.

Site	ARCSyM-3D elevation	Measured elevation
1. Imnavait/Upper Kuparuk	1300 m	914 m/754 m
2. Sagwon	554 m	300 m
3. West Kuparuk	369 m	152 m
4. Franklin Bluffs	349 m	83 m
5. Betty Pingo/Lower Kuparuk	0 m	12/15 m

resulting surface temperature was then used as a boundary condition for the subsurface model when calculating thaw depth and soil temperatures.

The initial step in analyzing the spatially distributed thermal processes is to develop the areally distributed meteorological datasets needed to solve the equations that describe the surface energy balance. This model uses data at a regular array of surface nodes spanning a large area ($>28\,000$ km^2). Seven identical meteorologic stations (see Table 2) located across the Kuparuk watershed were used to collect meteorologic data in a 10-m profile above the ground (LAII Science Steering Committee 1997). These data included precipitation, air temperature, relative humidity, wind speed and direction, incoming and reflected shortwave radiation, atmospheric and emitted longwave radiation, net radiation, and soil temperature. These data were distributed across the spatial domain using a kriging routine (Hinzman et al. 1998). Air temperature was adjusted (using the standard wet or dry adiabatic lapse rates according to conditions) to include the effects of elevation. Net radiation was adjusted to include effects of terrain aspect and slope.

2) REGIONAL CLIMATE MODEL

ARCSyM (Lynch et al. 1995) is a limited-area mesoscale climate model that incorporates representations of the atmosphere, land surface, sea ice, and ocean. The ARCSyM model is forced at the lateral boundaries and develops its own climate within the model domain. The lateral forcing, which includes temperature, wind, moisture, sea level pressure, and pressure heights, is obtained from European Centre for Medium-Range Weather Forecasts (ECMWF) observational analyses, and is updated every 12 h, at every vertical level. The land surface model employed in this study was the NCAR LSM (Bonan 1996), which includes a seasonally varying vegetation-canopy layer, a six-layer one-dimensional soil thermal and hydrological process parameterization, and a multiple surface type mosaic approach. Further details of this model can be found in Lynch et al. (1995) and Lynch et al. (1998).

The simulation presented here used 23 levels in the vertical with highest resolution in the boundary layer, and a 20-km horizontal grid resolution. The domain, centered on the North Slope of Alaska, measured 1500 km longitudinally and 900 km latitudinally (see Fig. 1). The sea ice model was run in ''thermodynamics-only'' mode, with ice dynamics switched off and ice concentration specified throughout the experiment based on Special Sensor Microwave Imager (SSM/I) data. Ice thickness was predicted by the ice thermodynamics model but ice concentration was forced to remain consistent with the SSM/I observations. The ocean model was replaced by a simple ''swamp'' formulation. This strategy was chosen to minimize any model biases that may arise from the nonland portions of the domain. This simulation, designated throughout the text as ARCSyM-3D, was performed with this model for the period April–September 1995, and used the generic vegetation types as used in the NCAR CCM3 model (Kiehl et al. 1996), but a high-resolution vegetation map was used where information was available.

A column version of ARCSyM has been developed that includes all the physical processes in the atmosphere and land surface, but uses observed winds, surface pressure, and temperature and moisture advection. This model can be implemented at a specific observational site for intercomparisons (e.g., Pinto et al. 1999) and in tests behaves very similarly to the full three-dimensional coupled model system. The advantages of this approach are the ability to target a specific site, the lack of model bias encroaching on results from that site, the ability to customize site characteristics, and the computational efficiency of the column approach. Simulations with this model using ECMWF analyzed forcing fields were performed at the Betty Pingo and Sagwon sites, for the period April–September 1995, and are designated ARCSyM-1D in the text. Nominal column horizontal resolution was 20 km, with 23 levels in the vertical, as in the spatially explicit simulations described above. These simulations differ from the spatially explicit experiments in that vegetation characteristics were modified based on available measurements of vegetation characteristics at the sites.

c. Synthesis of results

From the observations described in section (a), results for the two sites of interest have been extracted and monthly means have been constructed for the summer of 1995. Table 1 indicates the number of days of observations that go into each set of means. The monthly mean surface energy balance is shown in Tables 3 and 4, and charts for Betty Pingo in July and Sagwon in June are shown in Figs. 3 and 4, respectively—these months were chosen since they are representative and contain data from as many different measuring programs as were available.

Net radiation declined through the growing season at both coastal and upland sites, with high net radiation in June being similar between coastal and upland sites (Tables 3, 4), due to low solar zenith angle and infrequent cloudiness. On average, radiation declined earlier and more gradually in the upland (July) than the coastal

TABLE 3. Monthly mean surface energy balance at the coastal sites for (a) Jun, (b) Jul, and (c) Aug. The Barrow data from Ohmura (1982b) is a climatology for 1957–71. All values in W m^{-2}. Missing data (NA).

	Net radiation	Sensible heat flux	Latent heat flux	Ground heat flux
(a) Betty Pingo (Jun)				
Chapin and Eugster	NA	NA	NA	NA
Kane and Hinzman	128.1	39.6	61.0	27.5
Oechel and Vourlitis	124.9	43.0	39.6	40.5
England and Kim	NA	NA	NA	NA
Active-layer model	129.9	12.9	66.2	48.7
ARCSyM-1D	134.3	84.1	15.9	34.4
Ohmura Barrow climatology	116.9	41.7	40.5	15.1
(b) Betty Pingo (Jul)				
Chapin and Eugster	120.7	46.7	33.2	40.8
Kane and Hinzman	122.6	57.2	38.1	27.3
Oechel and Vourlitis	107.1	51.9	50.2	26.7
England and Kim	NA	NA	NA	NA
Active-layer model	123.4	13.2	76.5	28.9
ARCSyM-1D	128.8	51.9	78.2	−1.3
Ohmura Barrow climatology	130.8	57.9	64.8	8.1
(c) Betty Pingo (Aug)				
Chapin and Eugster	NA	NA	NA	NA
Kane and Hinzman	75.7	14.7	48.6	12.4
Oechel and Vourlitis	68.2	33.3	22.6	10.1
England and Kim	NA	NA	NA	NA
Active-layer model	74.4	17.1	48.2	9.9
ARCSyM-1D	66.0	37.1	28.9	0.1
Ohmura Barrow climatology	75.2	26.6	43.9	5.8

(August) sites. This is not typical of these sites for other years, but in 1995, precipitation was more frequent at the upland site (e.g., see Figs. 7 and 8) leading to an earlier greening. Like net radiation, sensible heat flux generally declined through the growing season in both sets of sites. There was no consistent difference in sensible heat flux between the coastal and upland sites in any month. In contrast, latent heat flux increased from June to July, then declined in August, paralleling the seasonal pattern of leaf area development. This seasonal pattern of evapotranspiration matches field measurements collected on the coastal plain (Mendez et al. 1998) and in the foothills (Kane et al. 1990). Latent heat flux was higher in upland than coastal sites during July and August, paralleling site differences in leaf area and air temperature. Sensible heat flux was generally similar to or slightly larger than latent heat flux throughout the summer at the coastal sites (Bowen ratio generally less than 1.5, although ranging as high as 1.9; Fig. 5a). These Bowen ratios were generally higher than climatologies from Hudson Bay (0.4–0.6; Lafleur and Rouse 1995) and, to a lesser extent, Barrow (0.6–1.0; Ohmura 1982b). In the upland site, Bowen ratio declined to around 0.7 during July and August (Fig. 5b), due to both increased latent heat flux and decreased sensible heat flux. Ground heat flux was highly variable among individual measurement sites and showed no consistent patterns other than a decline from July to August, particularly in the coastal sites.

Surface fluxes differed substantially among individual measurement sites within a region and season, reflecting differences in site properties, period of measurement, and methodology. For example, the Oechel sensible and latent heat fluxes are generally higher than

TABLE 4. Monthly mean surface energy balance at the upland sites for (a) Jun, (b) Jul, and (c) Aug. All values in W m^{-2}. Missing data (NA).

	Net radiation	Sensible heat flux	Latent heat flux	Ground heat flux
(a) Sagwon (Jun)				
Chapin and Eugster	58.4	31.2	26.3	13.8
Kane and Hinzman	120.8	21.3	80.2	19.3
Oechel and Vourlitis	114.3	47.8	38.9	23.0
England and Kim	126.4	NA	NA	8.8
Active-layer model	113.9	−15.2	94.0	36.3
ARCSyM-1D	150.5	57.9	56.6	36.0
(b) Sagwon (Jul)				
Chapin and Eugster	NA	NA	NA	NA
Kane and Hinzman	110.5	37.5	53.3	19.7
Oechel and Vourlitis	103.0	38.9	57.0	15.7
England and Kim	105.8	NA	NA	7.1
Active-layer model	105.8	−16.0	93.6	25.7
ARCSyM-1D	137.7	51.2	74.9	11.6
(c) Sagwon (Aug)				
Chapin and Eugster	NA	NA	NA	NA
Kane and Hinzman	73.0	26.0	37.7	9.2
Oechel and Vourlitis	70.0	27.8	41.5	10.6
England and Kim	94.2	NA	NA	3.4
Active-layer model	73.0	−1.3	56.7	16.3
ARCSyM-1D	70.9	36.1	32.5	2.3

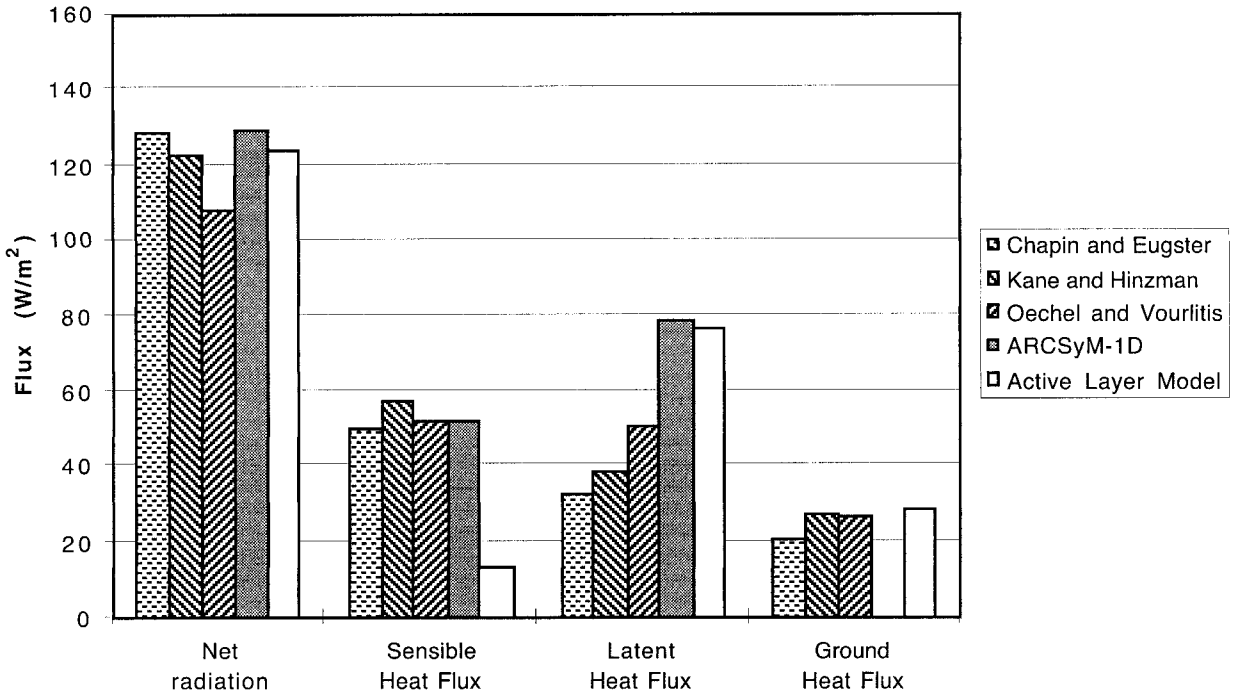

FIG. 3. Surface energy balance components as measured at the coastal sites (Betty Pingo), averaged over available observations in Jul.

all other data, sometimes by as much as 300%, although the Bowen ratios are often comparable. Spread in the ground heat flux measurements is large at the upland site (up to 430%) but quite close at the coastal site. In addition, the measuring programs approached energy balance closure to differing degrees—based on the monthly means, the energy balance closure for each group as a percentage of net radiation is

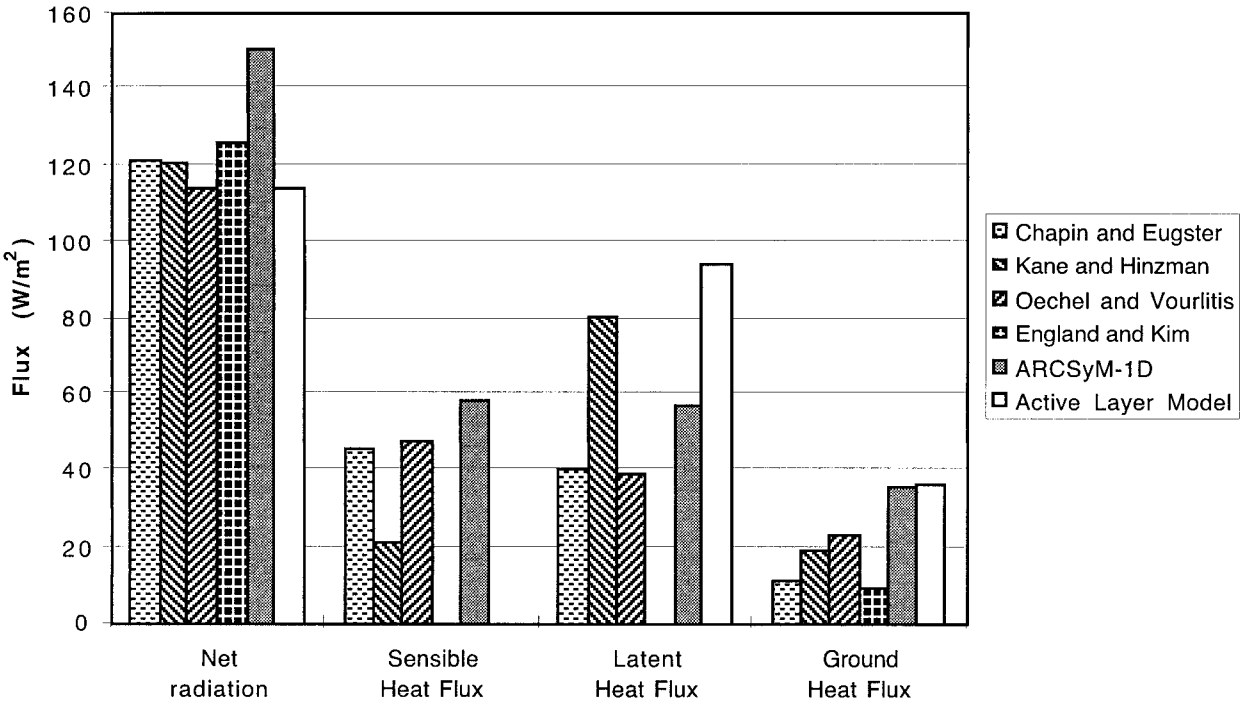

FIG. 4. Surface energy balance components as measured at the upland sites (Sagwon), averaged over available observations in Jun.

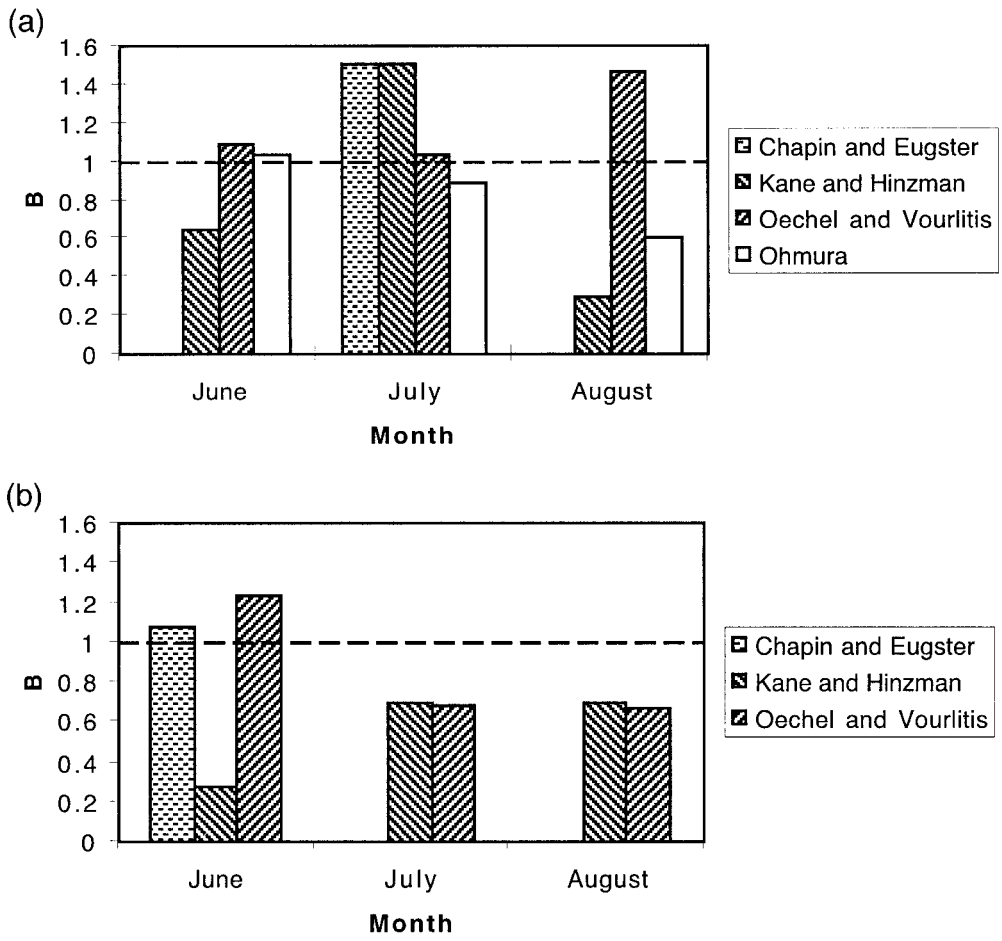

FIG. 5. Monthly mean Bowen ratios (a) for the coastal sites, and (b) for the upland sites, for available data.

- Chapin and Eugster: 0%–22%,
- Kane and Hinzman: 0%–3%,
- Oechel and Vourlitis: 1%–22%,
- Ohmura: 1%–17%.

This large variability among sites indicates the need for caution in interpreting small differences in fluxes within or among sites. Some of these site differences we can explain. For example, differences in net radiation measured by Kane's group and Oechel's group probably reflect true site differences in albedo or longwave emittance, since they used similar equipment and methods but the individual measurement sites were separated by about 50 m. The lower June net radiation measured by Chapin in the upland radiation reflects the greater frequency of cloudiness during their late June measurement period; the differing values of net radiation measured by England could reflect not only site dissimilarities but an additional methodological variation due to the use of different instruments. The large differences in ground heat fluxes among the upland sites reflect both true site differences (large differences in ground heat flux among microhabitats) and difficulties in getting good contact between heat flux plates and soil in the loose organic soils at these sites. In general, differences in fluxes were at least as great between investigators using similar instrumentation as between investigators using different instruments, suggesting that methodological differences were not the prime cause of variability among sites.

d. Modeling results

Model validation is generally achieved by performing comparisons between specific field data and model results at a grid point, or by comparing model simulations to extrapolations of groups of field data. Both of these approaches have inherent problems associated particularly with heterogeneity and scale. In this section we show the results of some strongly different modeling efforts in the context of the synthesis presented above. Tables 3 and 4 also show the results of simulations by the active-layer model and column experiments with ARCSyM-1D for the coastal (Betty Pingo) and upland (Sagwon) sites. Both of these sets of results use a single point in each model—in the ARCSyM-1D case this is

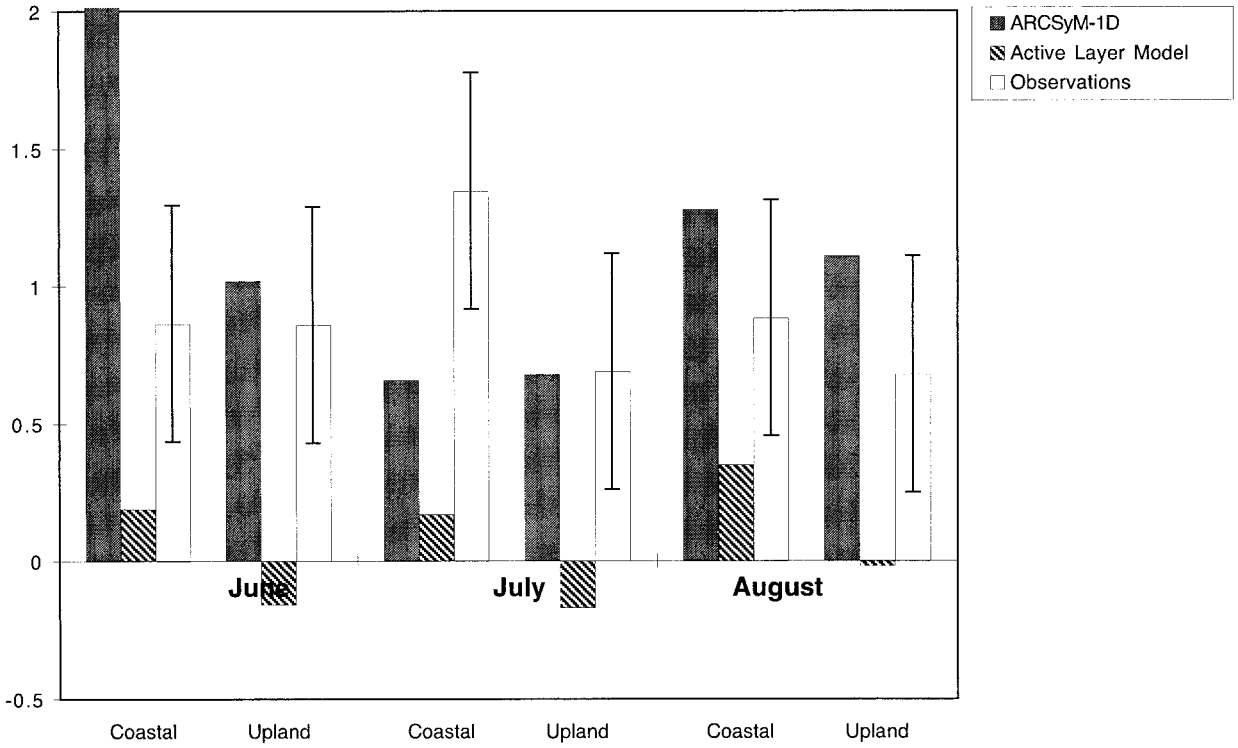

FIG. 6. Monthly mean Bowen ratios for the ARCSyM-1D and active-layer model, compared to an average of the observed mean Bowen ratio. Error bar represents one standard deviation of all measurements.

a column experiment performed at the site; in the case of the active-layer model, the grid cell encompassing the experimental site was used. The generic GCM tundra type employed by ARCSyM-1D was modified in each case. At the coastal site, changes were made to represent wet meadow characteristics. Changes to specifications included an aerodynamically smoother soil with decreased visible albedo and increased near-infrared (NIR) albedo, aerodynamically smoother vegetation with shorter stature, decreased leaf and stem area indices, larger leaves, and decreased root biomass. At the upland site, tussock tundra was present, with soils of similar characteristics to the wet meadow. Leaf and stem area indices and canopy height were increased in comparison to the wet meadow, though still not as large as the generic tundra type. Aerodynamic roughness, leaf size, and root biomass were all decreased.

Considering first the ARCSyM-1D simulations, results for the coastal site in July and August indicate an acceptable net radiation at the surface leading to reasonable sensible heat fluxes but excessive latent heat fluxes, resulting in insufficient late summer ground heat flux and a cooling and drying of the soil in August. The Bowen ratio produced by the simulations improves in comparison to the range of observations as the season advances (Fig. 6). In June, the results show a Bowen ratio over 5, although the sum of turbulent fluxes leaving the surface is of approximately the correct magnitude. In July, the Bowen ratio at 0.6 is too small and should be greater than unity. Figure 7 shows the temperature and moisture time series for the lowest model level in the atmosphere (along with interpolated ECMWF analyses for this point and level) and for the highest model level in the land surface model (the top 10 cm of soil). The soil and atmospheric moisture reflect the results seen in the latent heat flux response. June is a dry month, with few precipitation events. Atmospheric moisture and temperature are very close to the ECMWF analyses, which provide the boundary conditions. In mid-July there are several strong precipitation events, which leads to increased volumetric soil moisture (up to 35% compared to 10% in June), increased latent heat fluxes, and increased lower-level atmospheric moisture. The temperature time series shows that upper soil and surface temperatures are generally higher than atmospheric temperature in June, but the surface temperature drops in response to evaporative cooling following the precipitation events, reducing the sensible heat fluxes. At first sensible heat fluxes become too small, but over time the accuracy improves. This behavior indicates that the model is not correctly simulating rapidly fluctuating conditions.

In the upland site, the ARCSyM-1D results are quite different. The slight tendency for the model to overestimate net radiation (see Fig. 3) is enhanced, with concomitant large turbulent fluxes of heat and moisture, although the Bowen ratios are in the correct range (Fig. 6), as are the ground heat fluxes. The active-layer depth

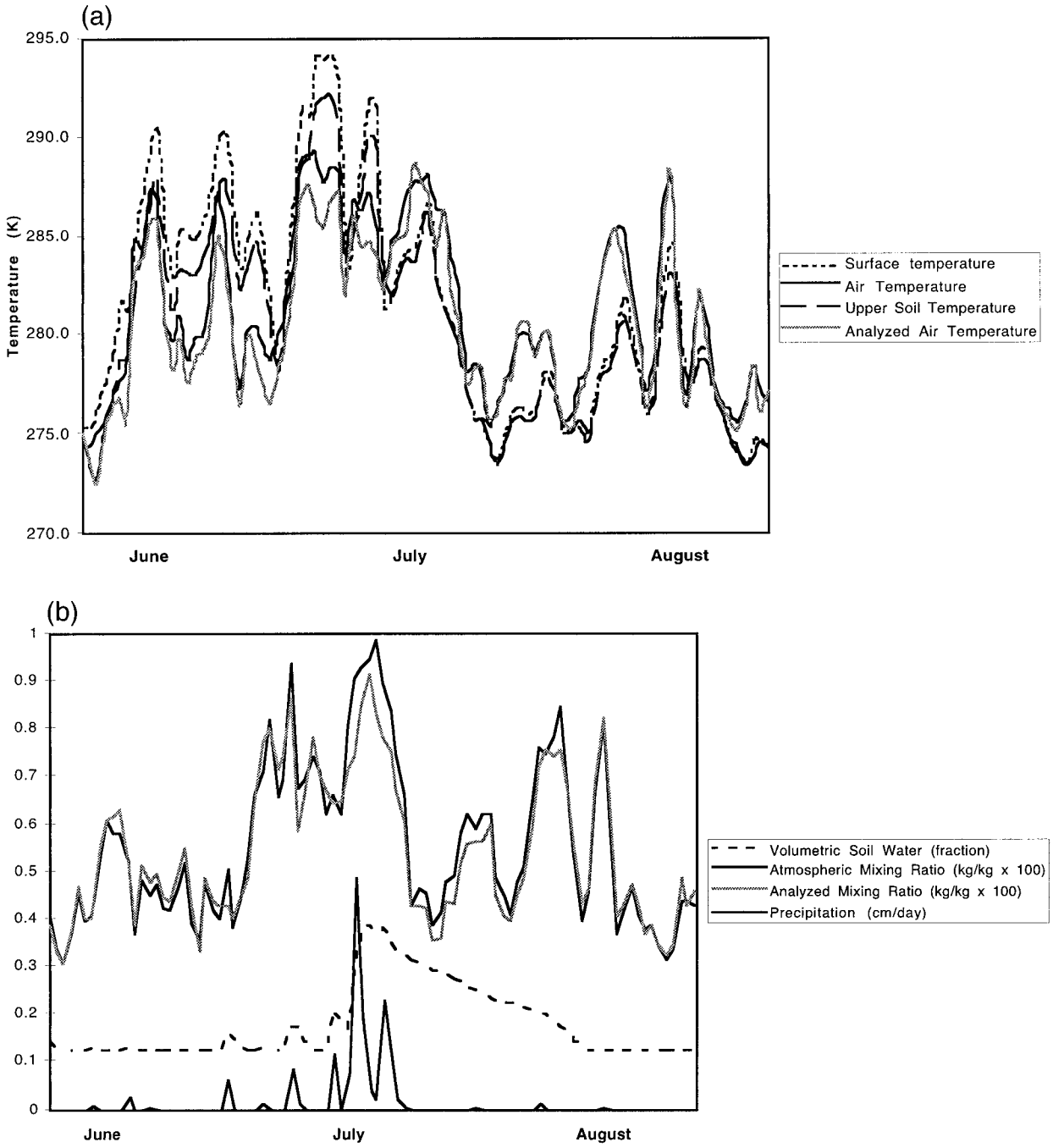

FIG. 7. Coastal (Betty Pingo) site—(a) temperature time series from ARCSyM-1D simulation, along with the atmospheric temperature at the same pressure height based on ECMWF large-scale analyses, and (b) moisture time series from ARCSyM-1D simulation, along with the atmospheric moisture mixing ratio at the same pressure height based on ECMWF large-scale analyses (units for each field noted in legend).

is much shallower than the coastal site, and soil temperatures and moisture generally vary within a smaller range. Soil moisture is generally higher (mean over the period of 35% compared to 17% at the coastal site) due to smaller, more regularly occurring precipitation events acting to keep the soil moist. Atmospheric temperatures and moisture mixing ratio closely follow the ECMWF analyses, and soil temperatures are generally lower (Fig. 8).

It would appear that, in the main, the model has a tendency to overestimate the turbulent fluxes of heat and moisture, and hence underestimate the ground heat flux available for warming the soil. In addition, the land surface model has difficulty adjusting to rapidly fluc-

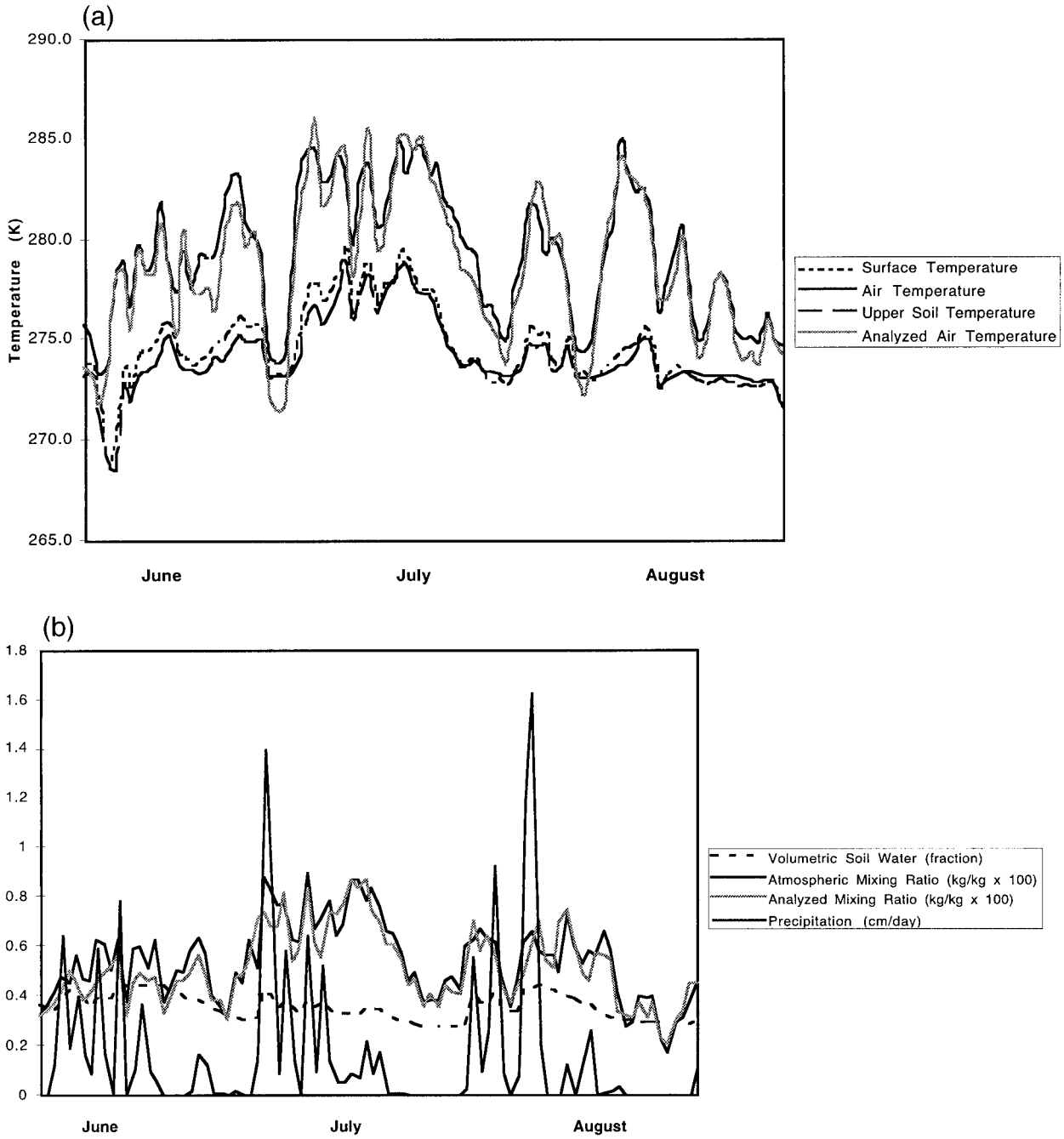

FIG. 8. Uplands (Sagwon) site—(a) temperature time series from ARCSyM-1D simulation, along with the atmospheric temperature at the same pressure height based on ECMWF large-scale analyses, (b) moisture time series from ARCSyM-1D simulation, along with the atmospheric moisture mixing ratio at the same pressure height based on ECMWF large-scale analyses (units for each field noted in legend).

tuating conditions. Despite this, the model demonstrates an ability to reproduce fairly accurate atmospheric profiles of temperature and moisture (see also Lynch et al. 1999).

Given the range of results from the various measurement programs, and the difficulty in initializing such a model experiment, the concordance with observations is quite high. The results reflect to an extent the tests of LSM in stand-alone mode performed by Tilley and Lynch (1998), which reproduced summer soil temperatures at Barrow and Imnavait with a high degree of accuracy but with soil moisture being underestimated. However, what was missing in those tests was interaction with the atmospheric column. Deficiencies in the land surface model simulation can be attributed primarily to the lack of an organic soil layer, representation

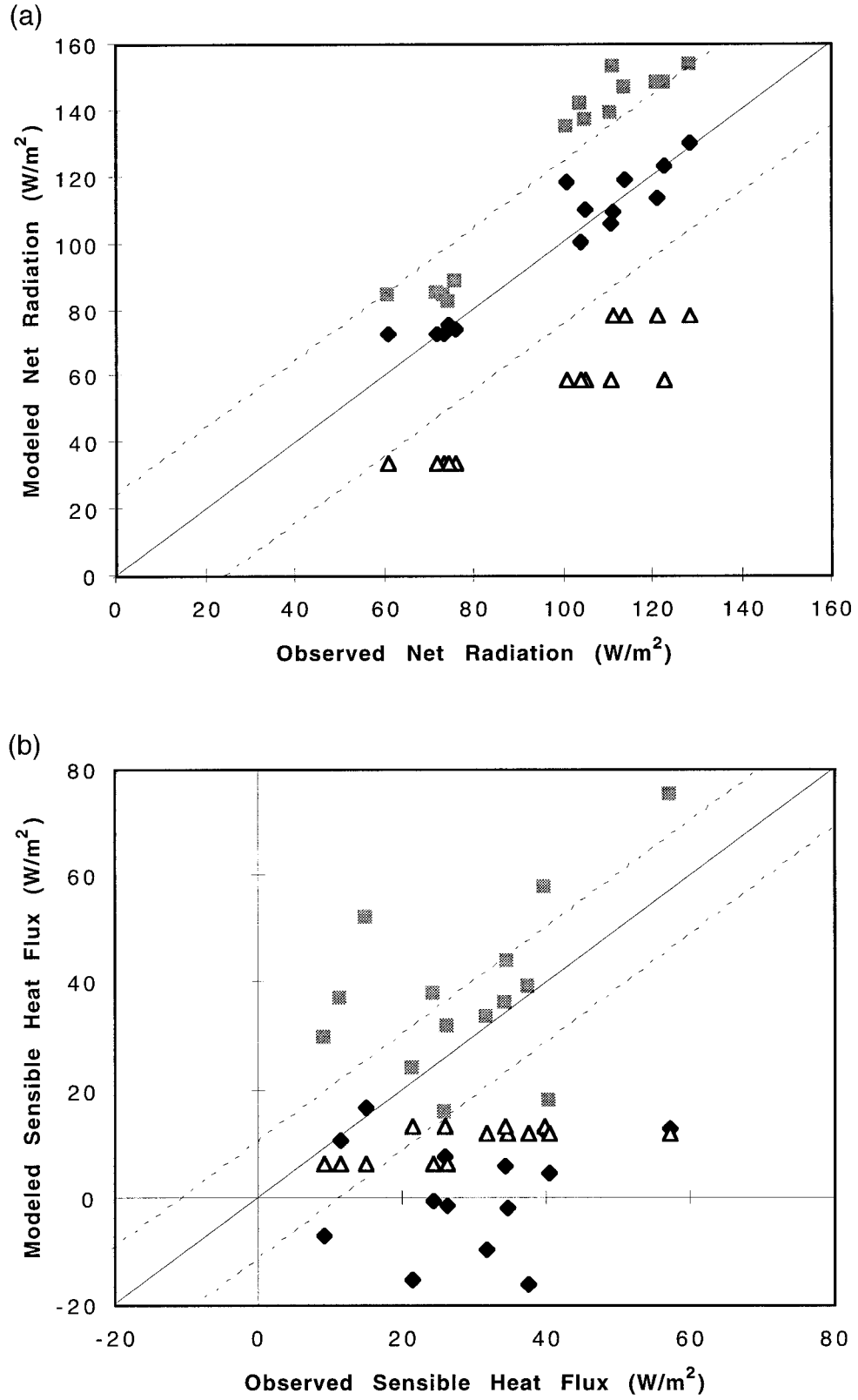

FIG. 9. Scatterplots showing the surface energy balance of the active-layer model (black diamonds), ARCSyM-3D (grey squares) and CCM3 (white triangles) compared to measurments made by the Kane and Hinzman group at three sites (Betty Pingo, Sagwon Hills, and Franklin Bluffs). The solid line indicates an exact

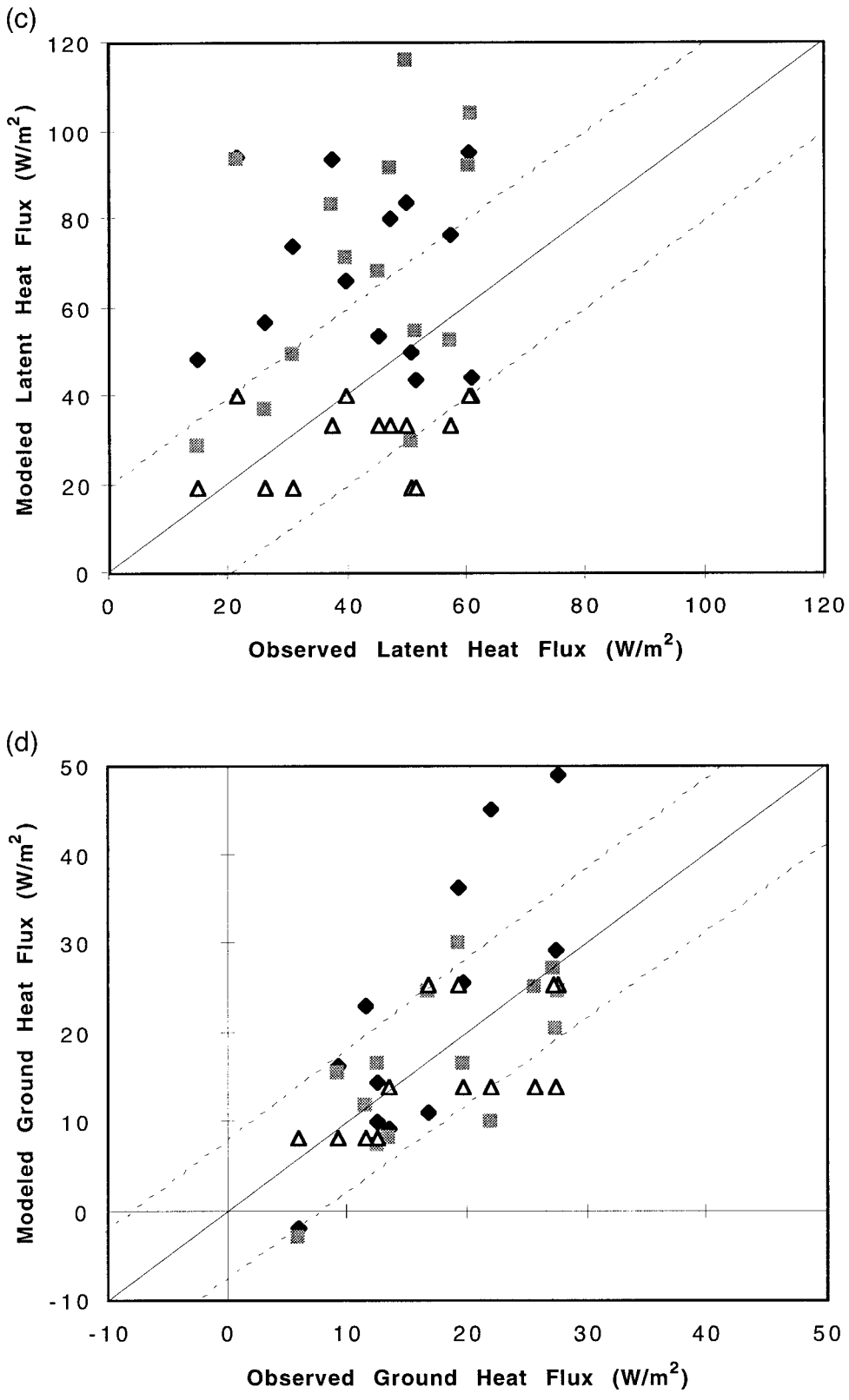

Fig. 9. (*Continued*) correspondence to the measurements, and the dashed lines indicate the expected uncertainty in the measurements based on the analysis of the observations in section 4c.

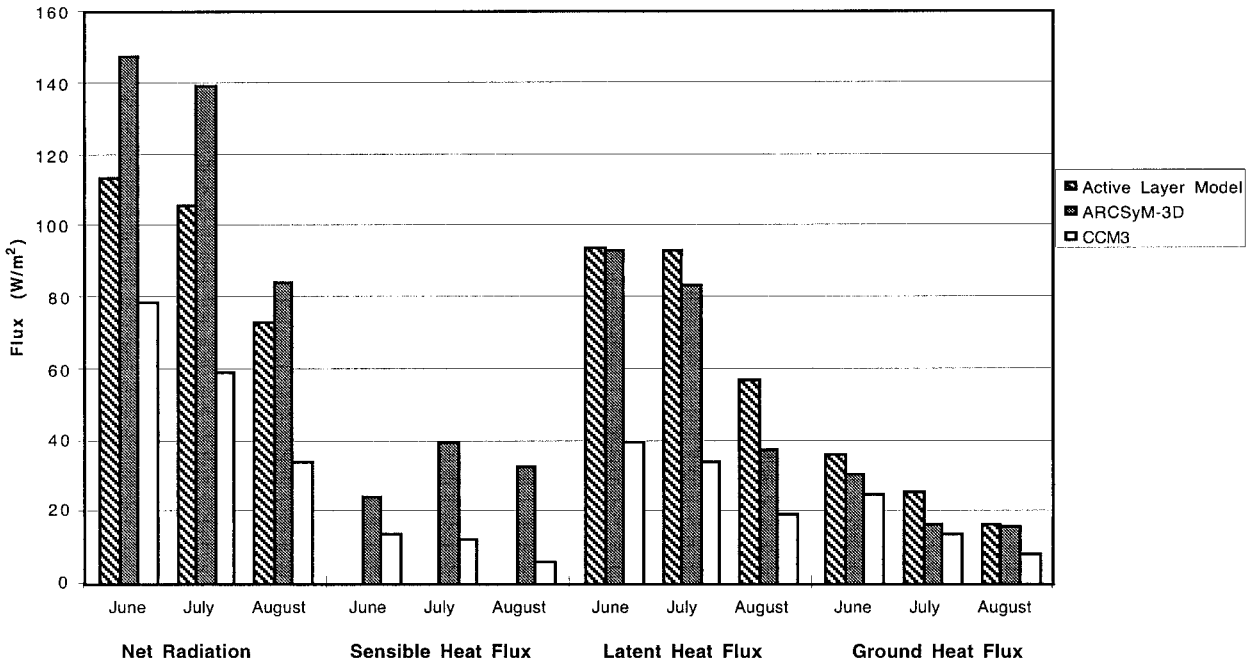

FIG. 10. Surface energy balance components for the Sagwon (upland) site for the active-layer model (area averaged over a 20 km × 20 km set of grid cells), ARCSyM-3D (a single grid cell covering a 400 km^2 region) and CCM3 (a single grid cell covering more than 60 000 km^2).

of mosses and oversimplified permafrost representation, which have a large impact on the ability of ARCSyM-1D to correctly model soil moisture and latent heat fluxes, although the soil temperatures are generally reasonable. Other deficiencies relate to the representation of net radiation and clouds in the atmospheric model, which leads to excessive energy available at the surface. We have not tuned the model to match observations, thus aiding identification of processes requiring improved representation in the model.

Turning to the active-layer model results, specific deficiencies are apparent. In particular, sensible heat fluxes are underestimated at the coastal sites and are negative at the upland sites, where no negative sensible heat fluxes are observed. Latent heat fluxes are generally comparable although showing a tendency to be slightly overestimated. The result is Bowen ratios outside the range of expected values in every case (Fig. 6). The problem is probably derived from the definition of where the surface temperature should be measured. This model was developed primarily to estimate active-layer dynamics. The optimum position to measure the surface temperature when calculating subsurface processes would be just below the surface vegetation, sheltered from solar radiation; however, the optimum position for determining sensible heat transfer would be a radiative measurement of the surface, including the vegetation and the stagnant air along the surface. This model considers the temperature of those two locations to be equal, leading to an underestimate of sensible heat. The active-layer model performance will be considered further, in comparison with spatially explicit ARCSyM-3D simulations.

We now turn to a comparison between the fluxes obtained from a spatially explicit ARCSyM-3D experiment (described in section 3) and 20 × 20 grid cell averages calculated from the higher resolution active-layer model. The scaling of turbulent fluxes from local to regional is an important problem. The usual approach is to area-weight average fluxes from various different land surface types occurring within a grid cell in a linear fashion, but this does not allow for micrometeorological variations or subgrid-scale changes in elevation and many other characteristics. Thus, by comparing models that use linear weighting, such as ARCSyM-3D and most GCMs, to a model that attempts to resolve these variations, we elucidate some of these important issues in scaling. ARCSyM-3D and the active-layer model are compared with a climatology from a state-of-the-art atmosphere–land GCM, the NCAR CCM3 model (Kiehl et al. 1996). Figure 1 shows the area covered by the CCM3 grid cell used, and a comparable regional climate model grid cell. The output from the active layer model, on a 1 km × 1 km grid, is averaged over the 20 × 20 grid cells surrounding each site. In cases where the two sites fall with a single ARCSyM-3D grid cell, these results are also averaged.

Table 2 lists the seven sites in the Flux Study region as mentioned in section 4b. In two cases, two of the sites are close enough together that they fall within a

single ARCSyM-3D model grid cell (20 km × 20 km), and hence they are grouped together. The first clear issue in this comparison is that of elevation (Table 2). The ARCSyM-3D model resolution creates a topography field by smoothing a higher resolution digital elevation map to the required spatial resolution (20 km × 20 km). In this case, the effect of smoothing is such that the apparent elevation is much higher than the actual elevation of the sites, often by more than 100%. The exceptions to this are the coastal sites, which, due to the smoothing of the coastline, are only just situated on land as far as the ARCSyM-3D model is concerned. The CCM3 grid cell, which encompasses all of these points, has an elevation of 474 m.

The results are compared with observations taken by the Kane and Hinzman group at several of these sites in Fig. 9. The figure shows a scatterplot of model results compared to the measurements for each of the energy balance components, and also indicates the likely uncertainty of the measurements based on the analysis in section 4c. Considering first the ARCSyM-3D and CCM3 results, it should be noted that these models use identical land surface model formulations but have some differences in the atmospheric representation. The CCM3 results are a climatology and hence can be compared also to the Ohmura Barrow climatology. In doing so, it is noted that the CCM3 climatology tends to overestimate net radiation, underestimate sensible and latent heat fluxes, and overestimate ground heat fluxes. When comparing the ARCSyM-3D and CCM3 results, immediately apparent is the horizontal resolution issue—given that the CCM3 grid box spans the entire region, it is unable to capture the local variations from one site to another. However, by falling within the range of values measured for these particular sites for the year 1995, the CCM3 model does capture the general response of ground and latent heat fluxes quite well. The sensible heat fluxes and net radiation tend to be underestimated when compared to the range of results from these sites. The ARCSyM-3D model, even at a relatively low resolution, performs quite well in capturing site differences, even though the detailed specifications of vegetation and soil type that were possible in the ARCSyM-1D column experiments were not possible in the spatially explicit experiment, which specified the same generic tundra type as CCM3. Again, a clear deficiency in the ARCSyM-3D experiment is a systematic positive bias in net radiation and turbulent fluxes. This overestimation is strongest early in the summer but there is no systematic site bias. Hence, in large part, the site to site variations seen in the ARCSyM-3D model are due to meteorological conditions and evolving site processes, rather than static site characteristics. Thus, while previous results with this model have indicated that the model is sensitive to the specification of land surface characteristics (Lynch et al. 1999), it cannot be concluded that these specifications are a major factor in model biases. Turning to the active layer model, due to the systematic underestimation of sensible heat flux discussed earlier, this model overestimates ground and latent heat fluxes over a broad area.

A selection of the results is also shown for a particular site in Fig. 10. The seasonal progression of decreasing total budget is observed in all models, and hence this large-scale forcing appears to be communicated at all scales. In the case of ARCSyM-3D, this leads to an overall decrease in all systematic biases as the season progresses. As we have seen in the column experiments, the sensible heat fluxes are higher for ARCSyM-3D than for the active-layer model, which tends to underestimate these fluxes. This result is also indicated in this case, where the sensible heat fluxes in the active layer model are of the same order of magnitude as the CCM3 results, and do not decrease as the season progresses. This result indicates that the subgrid scale variability of the active-layer model is of little utility to the large-scale since at this stage it does not indicate a great deal of skill. In this application, the broad linear weighting approach of the ARCSyM-3D performs quite adequately, and for detailed information is a clear improvement over the CCM3 results.

5. Summary

Differences in measured fluxes are due to a large number of factors, including instrument error and sampling issues, but it emerges that methodology differences and site differences contribute a comparable amount to the discrepancies. These models and analyses were prepared for complementary, but substantially different purposes and applications. In most cases, these analyses were conducted using independent datasets collected in the same general locations during the same general time period. The variability in the results depict the real differences in the surface energy balance that do exist across similar terrain, but also punctuate the fact that these differences cannot be correctly quantified unless similar techniques and equipment are employed.

The ARCSyM regional climate model performs adequately, but has difficulty with rapidly varying conditions, particularly those that affect soil hydrology. Comparing the ARCSyM results to a global model climatology, increasing horizontal resolution in the sub-Arctic appears to improve the simulation of the surface energy balance, with the exception of latent heat flux, which is clearly linked to the simulation of both precipitation and soil moisture. Correct simulation of the hydrologic cycle in climate models is crucial for long-term simulations, particularly with regard to vegetation dynamics and freshwater input to the oceans. The active-layer model generally overpredicts latent heat fluxes and underpredicts sensible heat transfer, yielding poor estimates of the Bowen ratio; while overestimating, it performs better at predicting soil heat flux as this is the primary application of this model.

General conclusions from this study confirm that the

summer climatology in this area of the Arctic is dominated by net radiation and latent heat fluxes. Sensible heat fluxes are also important during warmer, drier periods. In general, the ground heat flux represents about 10% of the net radiation. The spatial variability of fluxes is quite high, especially on the coastal plain where the landscape is nearly 50% shallow ponds, and the land areas gradate rapidly between very wet to somewhat dry.

Acknowledgments. The authors would like to thank the many investigators and students involved in collecting and processing the data for this synthesis. We also thank the two anonymous reviewers for their helpful comments. This work was supported in part by the National Science Foundation Arctic System Science Program through Grants OPP-9214810, OPP-9318535, OPP-9318532, and OPP-9523396.

REFERENCES

Ahrnsbrak, W. F., 1968: Summertime radiation balance and energy budget on the Canadian tundra. Tech. Rep. 37, Department of Meteorology, University of Wisconsin—Madison, 48 pp.

Alcamo, J., G. J. J. Kreileman, M. S. Krol, and G. Zuidema, 1994: Modeling the global society–biosphere–climate system. Part I: Model description and testing. *Water, Air Soil Pollut.,* **76,** 1–35.

Alley, R. B., 1995: Resolved: The Arctic controls global climate change. *Arctic Oceanography: Marginal Ice Zones and Continental Shelves Coastal and Estuarian Studies,* W. O. Smith and J. M. Grebmeier, Eds., Vol. 49, Amer. Geophys. Union, 263–283.

Avissar, R., and R. A. Pielke, 1989: A parameterization of heterogeneous land surfaces for atmospheric numerical models and its impact on regional meteorology. *Mon. Wea. Rev.,* **117,** 1113–2136.

Baldocchi, D., 1997: Measuring and modelling carbon dioxide and water vapour exchange over a temperate broad leaved forest during the 1995 summer drought. *Plant, Cell Environ.* **20,** 1108–1122.

Bergstrom, S., 1986: Recent development in snowmelt-runoff simulation. *Proc. Conf. on Cold Region Hydrology,* Fairbanks, AK, 461–468.

Beven, K. J., and M. J. Kirkby, 1979: A physically based, variable contributing area model of basin hydrology. *Hydro. Sci. Bull.,* **24,** 43–69.

Bonan, G. B., 1996: A land surface model (LSM Version 1.0) for ecological, hydrological, and atmospheric studies: Technical description and user's guide. NCAR Tech. Note NCAR/TN-417+STR, 150 pp.

——, D. Pollard, and S. L. Thompson, 1992: Effects of boreal forest vegetation on global climate. *Nature,* **359,** 716–718.

——, F. S. Chapin III, and S. L. Thompson, 1995: Boreal forest and tundra ecosystems as components of the the climate system. *Climate Change,* **29,** 145–167.

Bowers, J. D., and W. G. Bailey, 1989: Summer energy balance regimes for alpine tundra, Plateau Mountain, Alberta, Canada. *Arct. Alp. Res.,* **21,** 135–143.

Bromwich, D. H., R. Y. Tzeng, and T. R. Parish, 1994: Simulation of the modern Arctic climate by the NCAR CCM1. *J. Climate,* **7,** 1050–1069.

Chen, B., D. H. Bromwich, K. M. Hines, and X. Pan, 1995: Simulations of the 1979–1988 polar climates by global climate models. *Ann. Glaciol.,* **21,** 83–90.

Dickinson, R. E., A. Henderson-Sellers, and P. J. Kennedy, 1993: Biosphere–Atmosphere Transfer Scheme (BATS) version 1E as coupled to the NCAR Community Climate Model. NCAR Tech. Note NCAR/TN-387+STR, 72 pp.

Emanuel, W. R., H. H. Shugart, and M. P. Stevenson, 1985: Climatic change and the broad scale distribution of terrestrial ecosystem complexes. *Climate Change,* **7,** 29–44.

Eugster, W., J. P. McFadden, and F. S. Chapin III, 1997: A comparative approach to regional variation in surface fluxes using mobile eddy correlation towers. *Bound.-Layer Meteor.,* **85,** 293–307.

Everett, K. R., 1980: Soils and mapping. Environmental engineering and ecological baseline investigations along the Yukon River–Prudhoe Bay haul road. CRREL Rep. 80-19, 48–52. [Available from Cold Regions Research and Engineering Laboratory, U.S. Army Corps of Engineers, 72 Lyme Road, Hanover, NH 03755.]

Foley, J. A., J. E. Kutzbach, M. T. Coe, and S. Levis, 1994: Feedbacks between climate and boreal forests during the Holocene epoch. *Nature,* **371,** 52–54.

Goulden, M. L., B. C. Daube, S.-M. Fan, D. J. Sutton, A. Bazzaz, J. W. Munger, and S. C. Wofsy, 1997: Physiological responses of a black spruce forest to weather. *J. Geophys. Res.,* **102,** 28 987–28 996.

Graetz, R. D., 1991: The nature and significance of the feedback of changes in terrestrial vegetation on global atmospheric and climatic chnage. *Climate Change,* **18,** 147–,173.

Harazono, Y., M. Yoshimoto, G. L. Vourlitis, R. C. Zulueta, and W. C. Oechel, 1996: Heat, water and greenhouse gas fluxes over the arctic tundra ecosystems at Northslope in Alaska. *Proc. IGBP/BAHC-LUCC,* Kyoto, Japan, 170–173.

Hare, K. F., and J. C. Ritchie, 1972: Boreal bioclimates. *Geogr. Rev.,* **62,** 335–365.

Harvey, L. D. D., 1988a: Semi-analytic energy balance climate model with explicit sea ice and snow physics. *J. Climate,* **1,** 1065–1085.

——, 1988b: On the role of high latitude ice, snow and vegetation feedbacks in the climatic response to external forcing changes. *Climate Change.,* **13,** 191–224.

Henderson-Sellers, A., 1991: ''Incorporating'' vegetation and soil schemes into atmospheric general circulation models. Hydrological interactions between atmosphere, soil and vegetation. IAHS Publ. 204, 11–20.

——, and V. Gornitz, 1984: Possible climatic impacts of land cover transformation, with particular emphasis on tropical deforestation. *Climate Change,* **6,** 231.

Hinzman, L. D., and D. L. Kane, 1992: Potential response of an arctic watershed during a period of global warming. *J. Geophys. Res.,* **97** (D3), 2811–2820.

——, D. J. Goering, and D. L. Kane, 1998: A distributed thermal model for calculating temperature profiles and depth of thaw in permafrost regions. *J. Geophys. Res.,* in press.

Holdridge, L. R., 1964: *Life Zone Ecology.* Tropical Science Center, San Jose, Costa Rica.

Isard, S. A., and M. J. Belding, 1989: Evapotranspiration from the alpine tundra of Colorado, U.S.A. *Arct. Alp. Res.,* **21,** 71–82.

Kane, D. L., R. E. Gieck, and L. D. Hinzman, 1990: Evapotranspiration from a small Alaskan arctic watershed. *Nordic Hydrol.,* **21,** 253–272.

——, L. D. Hinzman, and J. P. Zarling, 1991: Thermal response of the active layer in a permafrost environment to climatic warming. *Cold Reg. Sci. Technol.,* **19,** 111–122.

Kiehl, J. T., J. J. Hack, G. B. Bonan, B. A. Boville, B. P. Briegleb, D. L. Williamson, and P. J. Rasch, 1996: Description of the NCAR Community Climate Model (CCM3). NCAR Tech. Note NCAR/TN-420+STR, 152 pp.

Kim, E. J., and A. W. England, 1995: Field data report for radiobrightness energy balance experiment 3 (9/94–9/95), Alaskan North Slope. University of Michigan Radiation Laboratory Rep. #RL-918, 17 pp.

Lafleur, P. M., and W. R. Rouse, 1988: The influence of surface cover and climate on energy partitioning and evaporation in a subarctic wetland. *Bound.-Layer Meteor.,* **44,** 327–347.

——, and ——, 1995: Energy partitioning at treeline forest and tundra

sites and its sensitivity to climate change. *Atmos.–Ocean,* **33,** 121–133.
——, ——, and D. W. Carlson, 1992: Energy balance differences and hydrologic impacts across the northern treeline. *Int. J. Climatol.,* **12,** 193–203.
LAII Science Steering Committee, 1997: Arctic system science land–atmosphere–ice interactions: A plan for action. Report to the National Science Foundation Office of Polar Programs Arctic System Science, 51 pp. [Available from LAII Science Management Office, University of Alaska, Fairbanks, AK 99775.]
Lynch, A. H., W. L. Chapman, J. E Walsh, and G. Weller, 1995: Development of a regional climate model of the western Arctic. *J. Climate,* **8,** 1555–1570.
——, D. L. McGinnis, and D. A. Bailey, 1998: The seasonal cycle and snow melt in a regional climate system model: Influence of land surface model. *J. Geophys. Res.,* **103,** 29 037–29 049.
——, G. B. Bonan, F. S. Chapin III, and W. Wu, 1999: The impact of tundra ecosystems on the surface energy budget of Alaska. *J. Geophys. Res.,* **104,** 6647–6660.
Maslanik, J. A., and Coauthors, 1996: An assessment of GENESIS v2.0 GCM performance for the Arctic. *Proc. ARCSS Modeling Workshop,* Boulder, CO.
Mather, J. R., and C. W. Thornthwaite, 1956: Microclimatic investigations at Point Barrow, Alaska, 1956. *Publications in Climatology,* Vol. 9, Drexel Institute of Technology, 51 pp.
——, and ——, 1958: Microclimatic investigations at Point Barrow, Alaska, 1957–1958. *Publications in Climatology,* Vol. 11, Drexel Institute of Technology, 239 pp.
Maykut, G., and Church, P. E., 1973: Radiation climate of Barrow, Alaska, 1962–66. *J. Appl. Meteor.* **12,** 620–628.
Mendez, J., L. D. Hinzman, and D. L. Kane, 1998: Evapotranspiration from a wetland complex on the arctic coastal plain of Alaska. *Nordic Hydrol.,* **29,** 303–330.
Monteith, J. L., 1965: Evaporation and environment. *Symp. Soc. Exp. Biol.,* **19,** 205–234.
Nobre, C. A., P. J. Sellers, and J. Shukla, 1991: Amazonian deforestation and regional climate change. *J. Climate,* **4,** 957–988.
Oechel, W. C., S. J. Hastings, G. Vourlitis, M. Jenkins, G. Riechers, and N. Grulke, 1993: Recent change of Arctic tundra ecosystems from a net carbon dioxide sink to a source. *Nature,* **361,** 520–523.
Ohmura, A., 1982a: A historical review of studies on the energy balance of arctic tundra. *J. Climatol.,* **2,** 185–195.
——, 1982b: Climate and energy balance on the Arctic tundra. *J. Climatol.,* **2,** 65–84.
——, 1984. Comparative energy balance study for arctic tundra, sea surface, glaciers and boreal forests. *Geo. J.,* **8,** 221–228.
Osterkamp, T., 1994: Evidence for warming and thawing of discontinuous permafrost in Alaska. *Eos, Trans. Amer. Geophys. Union,* **75,** 85.
Otterman, J., M. D. Chou, and A. Arking, 1984: Effects of nontropical forest cover in climate. *J. Climate Appl. Meteor.,* **23,** 762–767.
Pielke, R. A., and P. L. Vidale, 1995: The boreal forest and the polar front. *J. Geophys. Res.,* **100,** 25 755–25 758.
——, G. A. Dalu, T. J. Lee, H. Rodriguez, and T. G. F. Kittel, 1993: Mesoscale parameterization of heat fluxes due to landscape variability for use in general circulation models. Hydrological interactions between atmosphere, soil and vegetation. IAHS Publ. 212, 331–342.
Ping, C.-L., G. J. Michaelson, Y. Shur, and W. M. Loya, 1994: The genesis, classification and management of permafrost soils. Alaska soil geography field trip. University of Alaska, NMR 495-051, 56 pp. plus appendices. [Available from University of Alaska, Fairbanks, AK 99775.]
Pinto, J. O., J. A. Curry, and A. H. Lynch, 1999: Modeling clouds and radiation for the November 1997 period of SHEBA using a column climate model. *J. Geophys. Res.,* **104,** 6661–6678.
Pitman, A. J., 1991: The parameterization of sub-grid scale processes in climate models. Hydrological interactions between atmosphere, soil and vegetation. IAHS Publ. 204, 65–74.
Post, W. M., W. R. Emanuel, P. J. Zinke, and A. G. Stangenberger, 1982: Soil carbon pools and world life zones. *Nature,* **298,** 156–159.
Prentice, I. C., W. Cramer, S. P. Harrison, R. Leemans, R. A. Monserud, and A. M. Soloman, 1992: A global biome model based on plant physiology and dominance, soil properties and climate. *J. Biogeogr.,* **19,** 117–134.
Riseborough, D. W., and C. A. Burn, 1988: Influence of an organic mat on the active layer. *Proc. Fifth Int. Conf. on Permafrost,* Trondheim, Norway, Tapir Publ., 633–638.
Rott, H., and F. Obleitner, 1992: The energy balance of dry tundra in west Greenland. *Arct. Alp. Res.,* **24,** 352–362.
Rouse, W. R., D. W. Carlson, and E. J. Weick, 1992: Impacts of summer warming on the energy and water balance of wetland tundra. *Climate Change,* **22,** 305–326.
Rovansek, R. J., L. D. Hinzman, and D. L. Kane, 1996: Hydrology of a tundra wetland complex on the Alaskan arctic coastal plain. *Arct. Alp. Res.,* **28,** 311–317.
Sellers, P. J., Y. Mintz, Y. C. Sud, and A. Dalcher, 1986: A simple biosphere model (SiB) for use within general circulations models. *J. Atmos. Sci.,* **43,** 505–531.
Shaeffer, J. D., and E. R. Reiter, 1987: Measurments of surface energy budgets in the Rocky Mountains of Colorado. *J. Geophys. Res.,* **92,** 4145–4162.
Shaw, E. M., 1994: *Hydrology in Practice.* 3d ed. Chapman and Hall, 569 pp.
Smith, E. A., H. J. Cooper, W. L. Crosson, and W. Heng-yi, 1993: Estimation of surface heat and moisture fluxes over a prairie grassland 3. Design of a hybrid physical/remote sensing biosphere model. *J. Geophys. Res.,* **98,** 4951–4978.
Smith, T. M., and H. H. Shugart, 1993: The potential response of global terrestrial carbon storage to a climate change. *Water, Air Soil Pollut.,* **70,** 629–642.
Steffen, W. L., F. S. Chapin III, and O. A. Sala, 1996: Global change and ecological complexity: An international research agenda. *Trends Ecol. Evol.,* **11,** 186 pp.
Thomas, G., and P. R. Rowntree, 1992: The boreal forests and climate. *Quart. J. Roy. Meteor. Soc.,* **118,** 469–497.
Tilley, J. S., and A. H. Lynch, 1998: On the applicability of current land surface schemes for Arctic tundra: An intercomparison study. *J. Geophys. Res.,* **103,** 29 051–29 063.
Verseghy, D., 1991: CLASS—A Canadian land surface scheme for GCMs. Part I: Soil model. *Int. J. Climatol.,* **11,** 111–133.
——, N. A. McFarlane, and M. Lazaren, 1993: CLASS—A Canadian land surface scheme for GCMs. Part II: Vegetation model and coupled runs. *Int. J. Climatol.,* **13,** 347–370.
Vourlitis, G. L., 1997: Large-scale measurements of net CO_2 flux and energy balance of Alaskan arctic tundra ecosystems. Ph.D. dissertation, San Diego State University and the University of California, Davis, 146 pp.
——, and W. C. Oechel, 1997: Landscape CO_2, H_2O vapor and energy flux of moist-wet coastal tundra ecosystems over two growing seasons. *J. Ecol.,* **85,** 575–590.
Vowinckel, E., 1966: The surface heat budgets at Ottawa and Resolute, N. W. T. Arctic Meteorology Research Group, Department of Meteorology, McGill University, Publication in Meteorology 85, 27 pp.
Walker, M. D., D. A. Walker, and K. R. Everett, 1989: Wetland soils and vegetation, arctic foothills, Alaska. U.S. Fish and Wildlife Service, Biological Rep. 89 (7), 89 pp.
Walsh, J. E., and R. G. Crane, 1992: A comparison of GCM simulations of arctic climate. *Geophys. Res. Lett.,* **19,** 29–32.
Weller, G., and C. Benson, 1971: The structure and function of the tundra ecosystem. Progress Rep. 6, U.S. Tundra Biome Program, International Biological Program, and U.S. Arctic Research Program, Tundra Biome Center, 181 pp. [Available from University of Alaska, Fairbanks, AK 99775.]

——, and B. Holmgren, 1974: The microclimates of the arctic tundra. *J. Appl. Meteor.,* **13,** 854–862.
Wendler, G., 1967: The heat balance at the snow surface during the melting period March, April 1966 near Fairbanks, Alaska. *Gerlands Beitr. Geophys.,* **76,** 453.
Wetzel, P. J., and J.-T. Chang, 1988: Evapotranspiration from nonuniform surfaces: A first approach for short term numerical weather prediction. *Mon. Wea. Rev.,* **116,** 600–621.
Whalen, S. C., and W. S. Reeburgh, 1990: Consumption of atmospheric methane by tundra soils. *Nature,* **346,** 160–162.
Wilson, M. F., A. Henderson-Sellers, R. E. Dickinson, and P. J. Kennedy, 1987: Investigation of the sensitivity of the land surface parameterization of the NCAR Community Climate Model in regions of tundra vegetation. *J. Climatol.,* **7,** 319–343.
Woodward, F. I., 1987: *Climate and Plant Distribution.* Cambridge University Press, 253 pp.
Yoshimoto, M., Y. Harazono, A. Miyata, and W. C. Oechel, 1996: Micrometeorology and heat budget over the arctic tundra at Barrow, Alaska in the summer of 1993. *J. Agric. Meteor.,* **52,** 11–20.